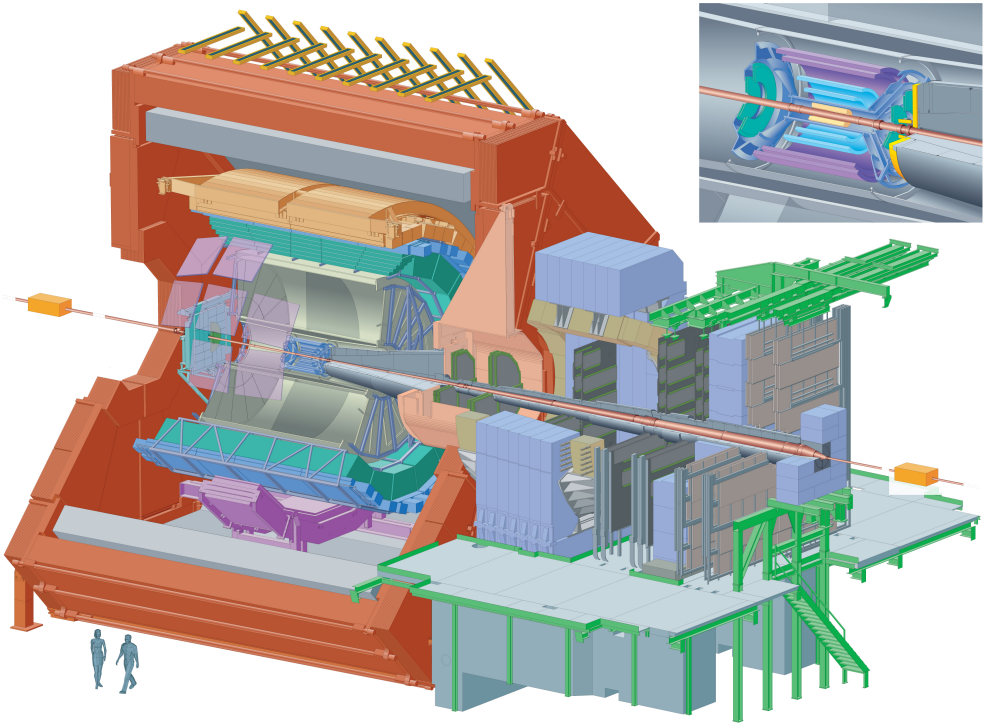

Inelastic and diffraction dissociation cross-sections in proton-proton collisions with ALICE

Martin Poghosyan

(CERN)

on behalf of the ALICE collaboration

CERN-PH LHC Seminar – 09/10/12

Outlook of the talk

- Diffraction
- History
- Regge theory
- Pomeron
- Unitarity effects
- Known knowns and known unknowns

- Inelastic and diffractive cross-sections measurements with ALICE

With non 4π-detectors we see a fraction of events in a limited phase-space

The challenge is to find out what we do not see.

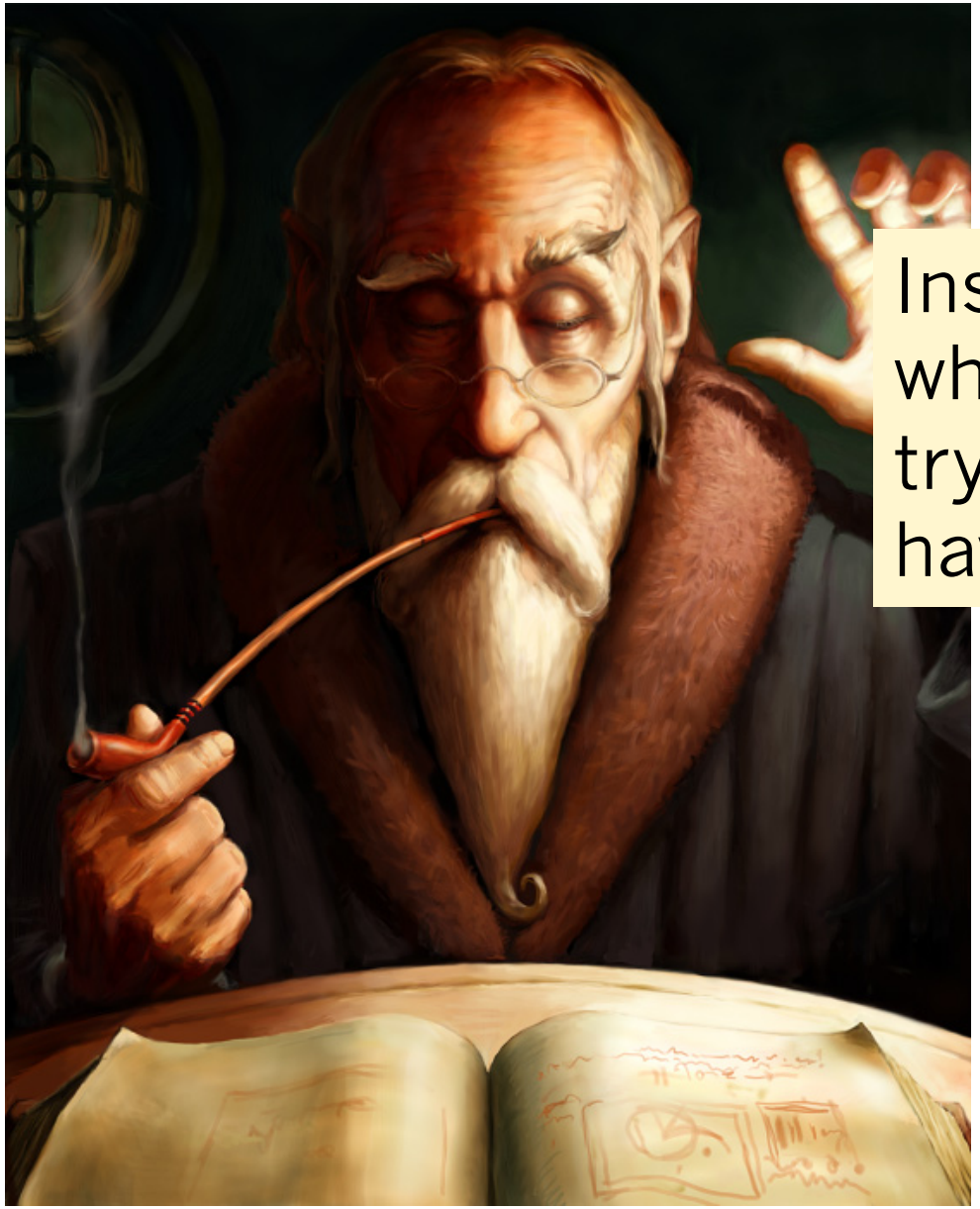

Instead of thinking about what we are missing, let's try to think about what we have.

A Lot of Interest Covering Experiment

Triggers:

- **V0 : $-3.7 < \eta < -1.7$ and $2.8 < \eta < 5.1$**
- **SPD : $|\eta| < 2$.**

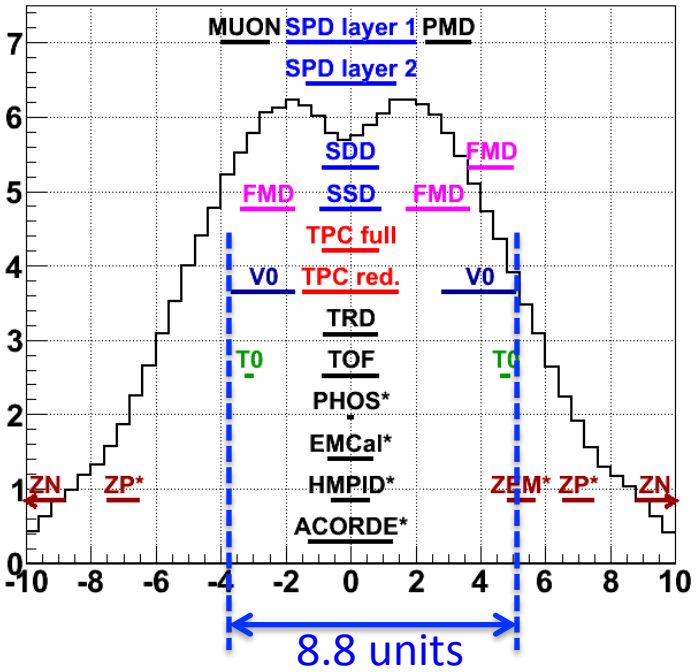

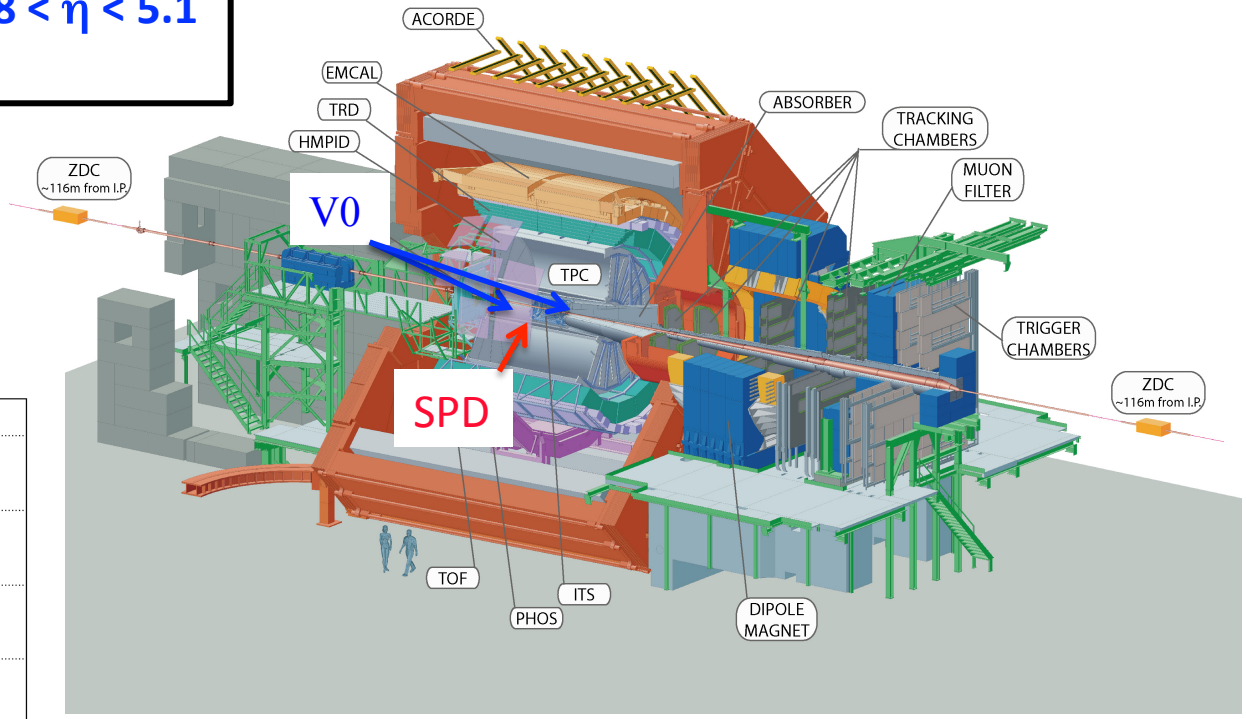

- High granularity
- Minimized material
- Good PID
- Good acceptance for p_t down ~20 MeV/c (hits)

Let's estimate the fraction of non-observed events by looking at the observed ones.

Minimum Bias (MB) triggers cover the η-range from -3.7 to 2 and from 2.8 to 5.1.

There are large rapidity-gap processes (diffractive) which we miss.

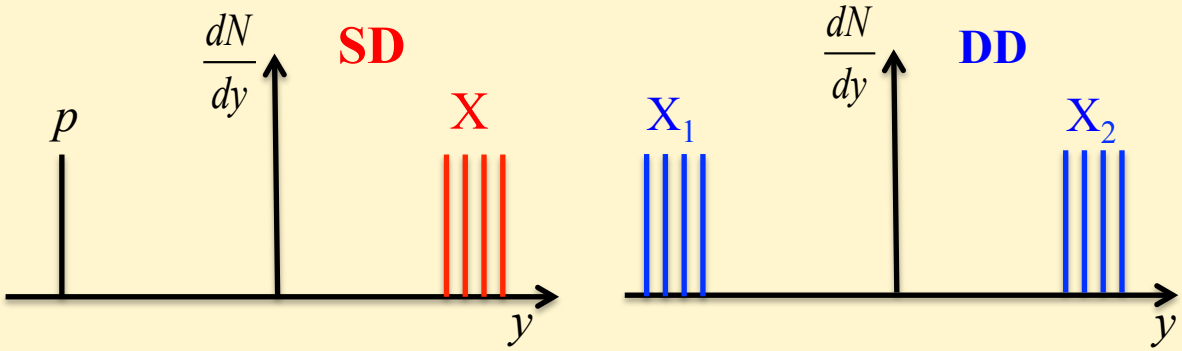

Coherence length/formation zone

The high-directivity radiation of relativistic particles is formed throughout a coherence length/formation zone (Ter-Mikaelyan 1953)

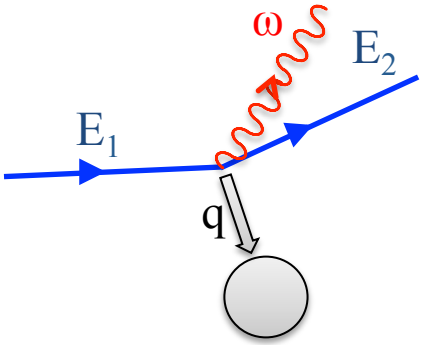

$$L_{coh} \equiv \frac{1}{q_{\parallel}} \approx \frac{2E_1E_2}{\omega m_e^2}$$

For large E_1 and/or small ω the L_{coh} can reach macroscopic dimensions.

It is the coherence length rather than the wavelength of the particle, that can be a measure of the size of the domain relevant for the effect.

This statement led to fundamental conclusions:

- Landau-Pomeranchuk effect (1953)
- Diffraction dissociation of hadrons (Pomeranchuk and Feinberg 1953)

"On external (diffraction) generation of particles in nuclear collisions"

Feinberg and Pomeranchuk noted that inelastic diffraction scattering can occur in all cases in which the coherence condition $R << L_{coh}\ (=1/q_{||})$ is satisfied. The target participates in the process as a whole.

$$\mathrm{N} + \mathrm{A} \rightarrow \mathrm{N} + \pi + \mathrm{A}$$

$$L_{coh} = \frac{E}{m_N m_\pi} \quad \Rightarrow \quad E >> m_N m_\pi R$$

($L_{coh} \approx$ 20 nm for p+Pb at $\sqrt{s_{NN}}$ = 5.02 TeV)

general case: $\mathrm{h} + \mathrm{A} \rightarrow \mathrm{h}^* + \mathrm{A}$

$$L_{coh} = \frac{2E}{m^{*2} - m^2} \quad \Rightarrow \quad E >> \left(m^{*2} - m^2\right) R \quad \Rightarrow \quad m^* >> m \quad \Rightarrow \quad m^* << \frac{1}{\sqrt{2mR}} \sqrt{s}$$

Spectra of particles in pp

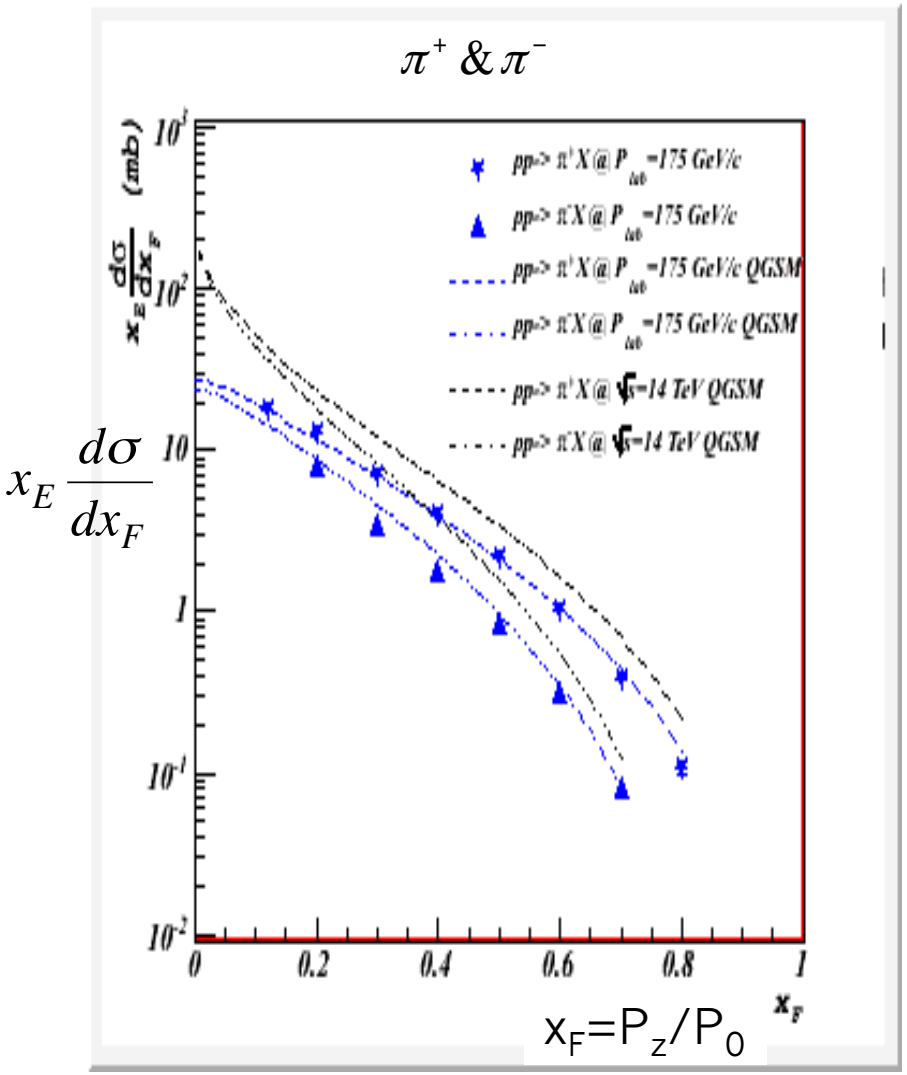

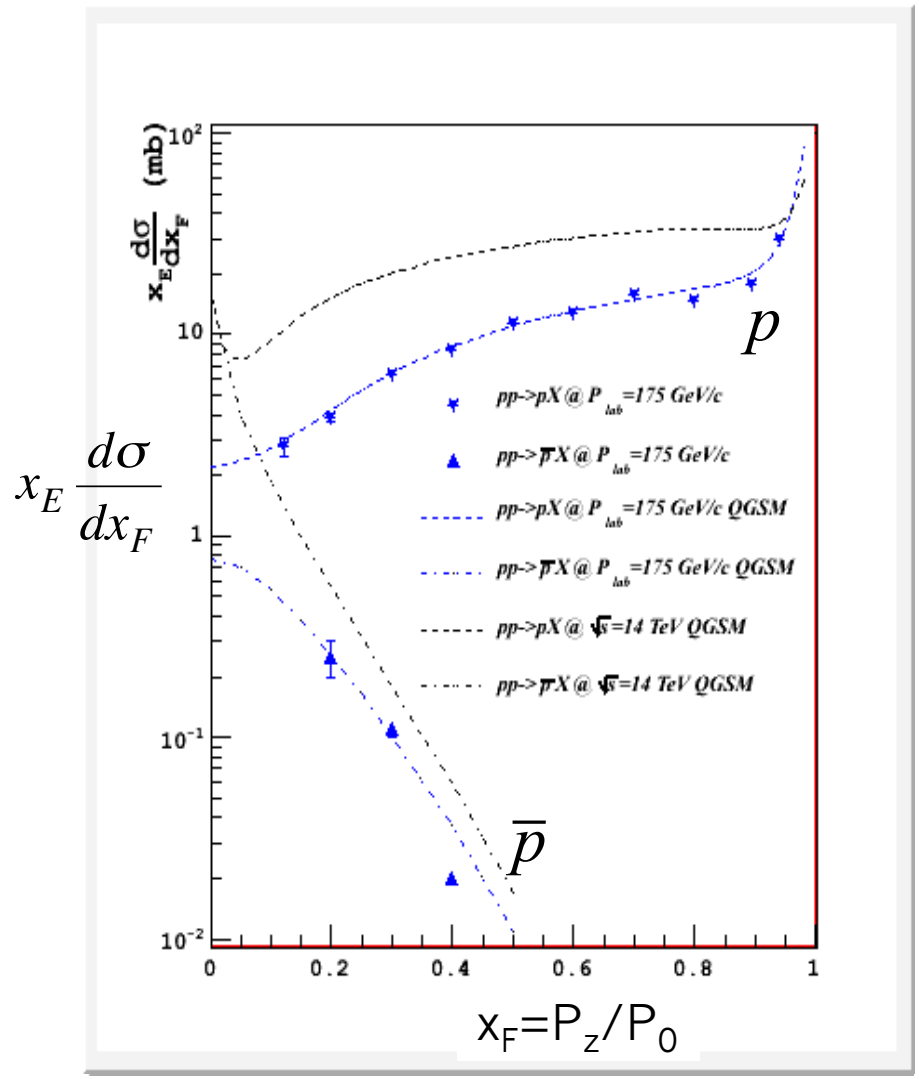

only the proton spectrum increases at $x_F \rightarrow 1$

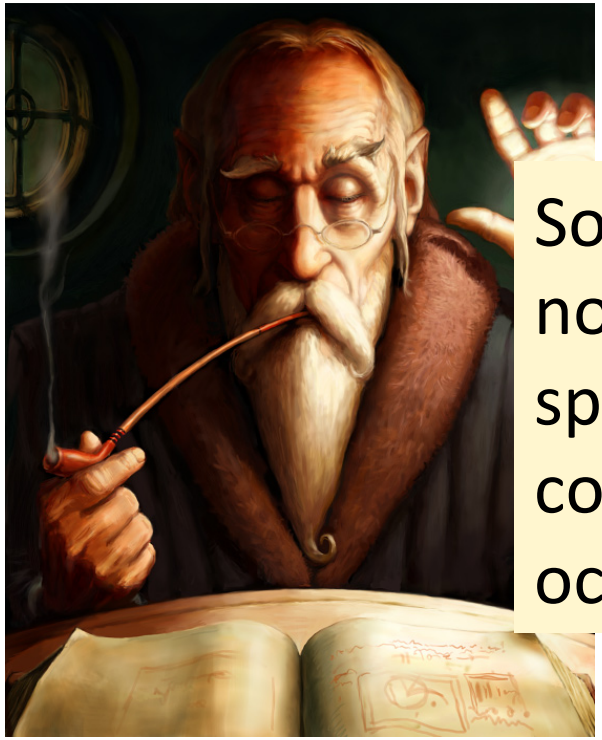

Some QED or QCD processes involve a non-local interaction. There is no way of specifying at what point within the coherence length the interaction occurred.

Space-time picture of hh/hA/AA interactions

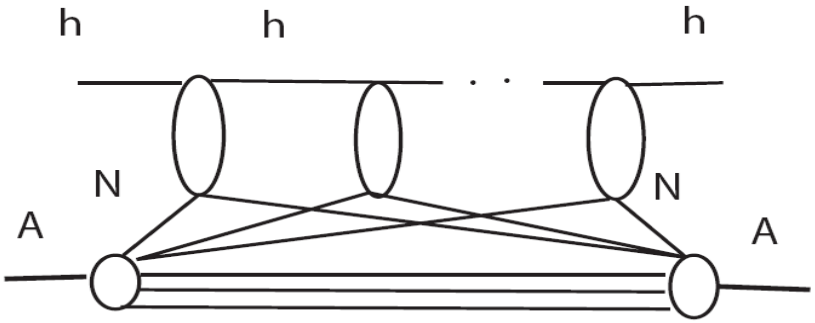

At low energies, $E < E_c$ ($E_c \sim mR$), an elastic *hA* –scattering can be considered as successive rescatterings of an initial hadron on nucleons inside a nucleus (Glauber).

For $E > E_c$ there is a coherent interaction of constituents of a hadron with nucleons of a nucleus. *hA* elastic amplitude can be calculated as in the Glauber model, but taking into account diffractive intermediate states (Gribov).

GRIBOV THEORY OF NUCLEAR INTERACTIONS AND PARTICLE DENSITIES AT FUTURE HEAVY-ION COLLIDERS .

A. Capella[a)], A. Kaidalov[a),b)] and J. Tran Thanh Van[a)]

Heavy Ion Phys. 9 (1999, published before the RHIC era!)

and LHC . Limitations of the Glauber approximation and its modification at high energy according to the Gribov theory will be discussed . It will be shown that these modifications are related to large mass diffraction dissociation of hadrons which leads to extra shadowing in the system. These effects reduce particle densities in the central rapidity region compared to the Glauber approximation predictions. This result is valid for both soft and hard processes. To estimate these shadowing effects we apply Gribov theory to the processes of deep inelastic scattering (DIS) on nuclei and show how it is possible to

For collisions of identical nuclei (SS, PbPb) the $A^{4/3}$–dependence of particle densities of eq. (10) typical for the Glauber model changes to the behaviour A^{δ}. The value of delta is a weak function of energy and it is equal to $\delta \approx 1.1$ at LHC energies.

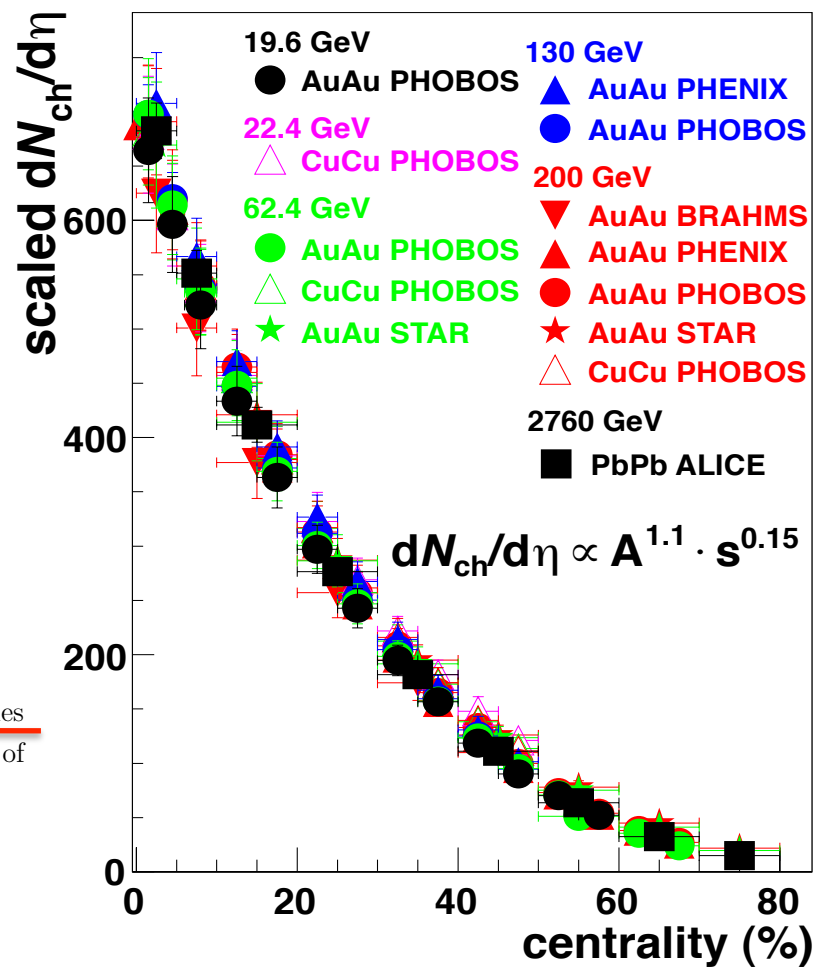

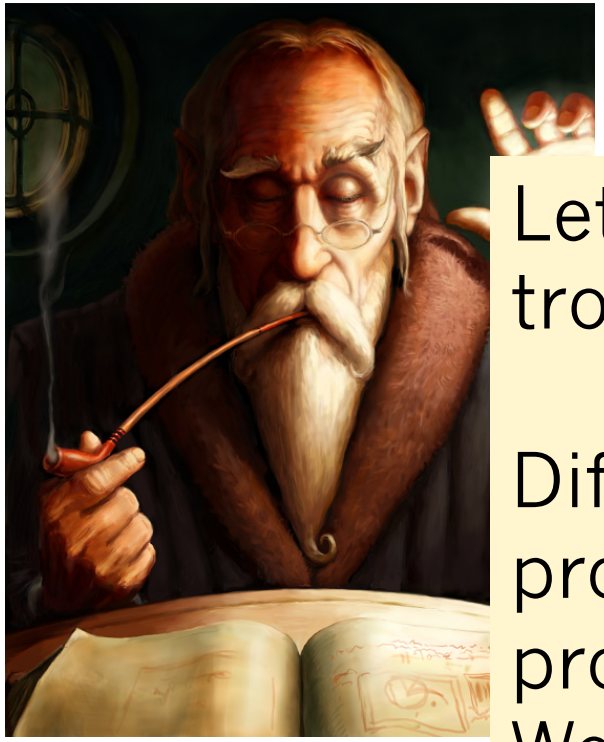

Let's not consider diffraction as only a trouble for detector effects correction.

Diffraction is a non-perturbative QCD process and QCD has major unsolved problems in this domain.
We can learn a lot!

This is why ALICE is interested in diffraction.

s-channel view of diffraction

(Good and Walker 1960)

For states ϕ_k which diagonalize the diffractive part of the T[=i(I-S)] matrix:

$$\mathrm{Im}T = CFC^T \quad \text{with} \quad \langle\varphi_j|F|\varphi_k\rangle = F_j\delta_{jk}$$

For an arbitrary incoming particle: $\left|i\right\rangle = \sum_k C_{ik}\left|\phi_k\right\rangle$

Elastic scattering amplitude: $\left\langle i\right|\mathrm{Im}\,T\left|k\right\rangle = \sum_k \left|C_{ik}\right|^2 F_k = \left\langle F\right\rangle$

$$\frac{d\sigma_{sd}}{d^2b} = \left\langle F^2\right\rangle - \left\langle F\right\rangle^2$$ dispersion of the eigenvalues distribution

In the case of a black disc ($F_k = 1$), diffraction is possible on its periphery:

$$\sigma_{tot}(s) \propto R^2(s) \propto \ln^2 s \qquad \sigma_{sd}(s) \propto R(s) \propto \ln s$$

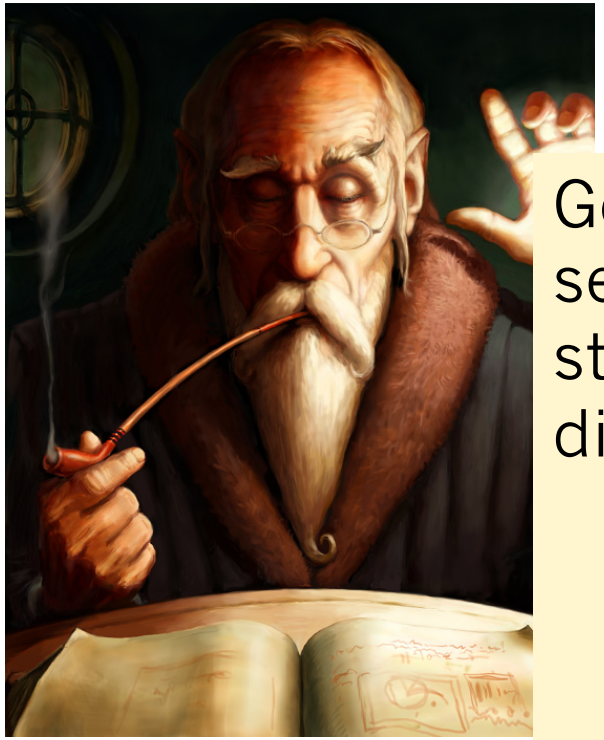

Good-Wolker approach assumes a separation of diffractive and inelastic states, which is not true for large mass diffraction.

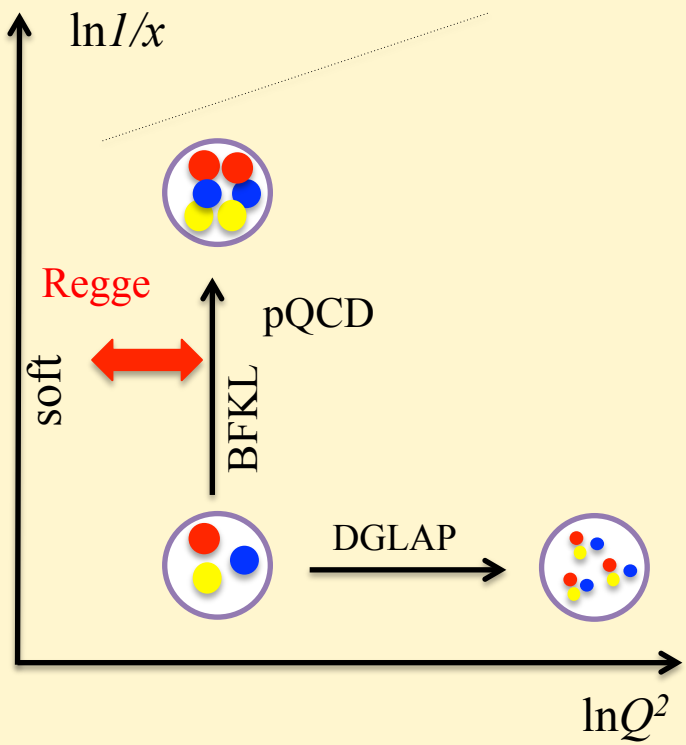

The Reggeon concept

t-channel exchange picture

Exchange by a particle with spin J in the t-channel

$$T(s,t) = \frac{g_{13}g_{24}}{t - m_J^2} s^J \quad \left(s >> m_i^2\right)$$

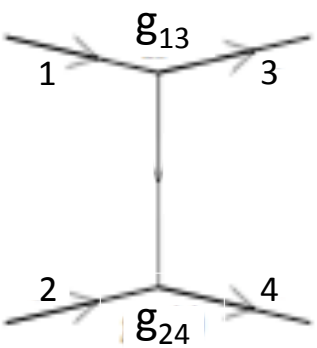

There are many particles (resonances) with spin $J > 1$!

$$T(s,t) = 2\sum_{l=0}^{\infty} f_l(t) P_l(z) = \frac{1}{2i}\int_C \frac{f(\alpha,t)P_\alpha(-z)}{\sin(\pi\alpha)} d\alpha$$

$$T(s,t) \propto \left(\frac{s}{s_0}\right)^{\alpha(t)}$$

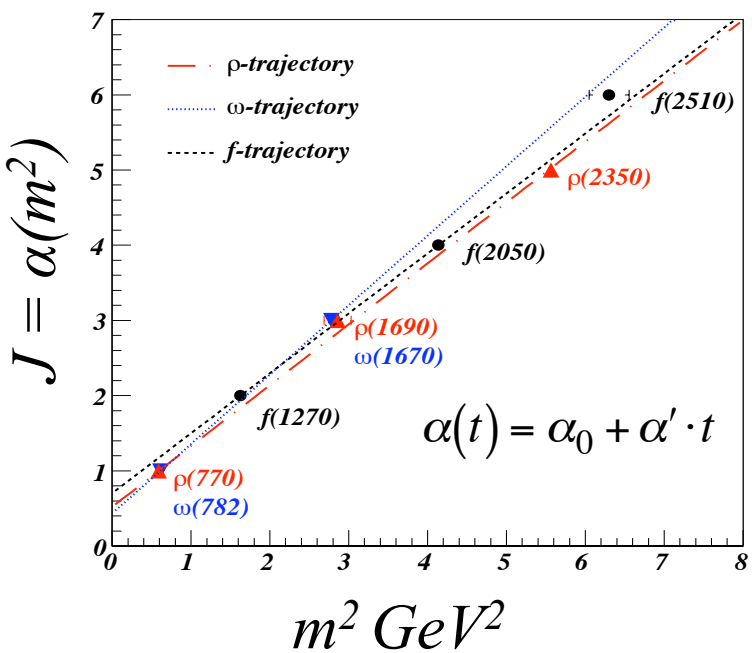

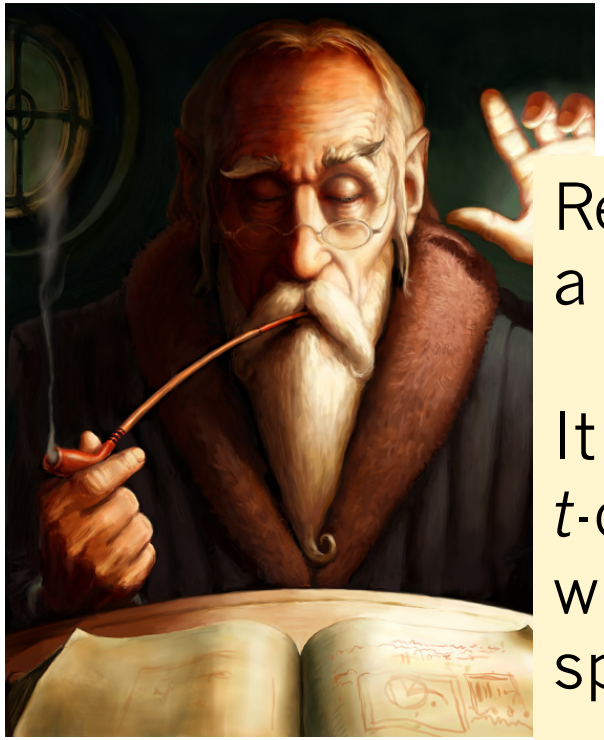

Regge pole theory is a generalization of a particle exchange in the *t*-channel.

It corresponds to an exchange in the *t*-channel by a state of "spin" $\alpha(t)$, which coincides with particles of spin J for $t = m^2_J$.

$$T(s,t) \propto \left(s / s_0\right)^{\alpha(t)}$$

$$\Downarrow$$

$$\sigma_{tot} \approx \frac{1}{s} \operatorname{Im} T(s,0) \propto s^{\alpha(0)-1}$$

$$\Delta \equiv \alpha(0) - 1 < 0 \quad ?$$

Pomeron

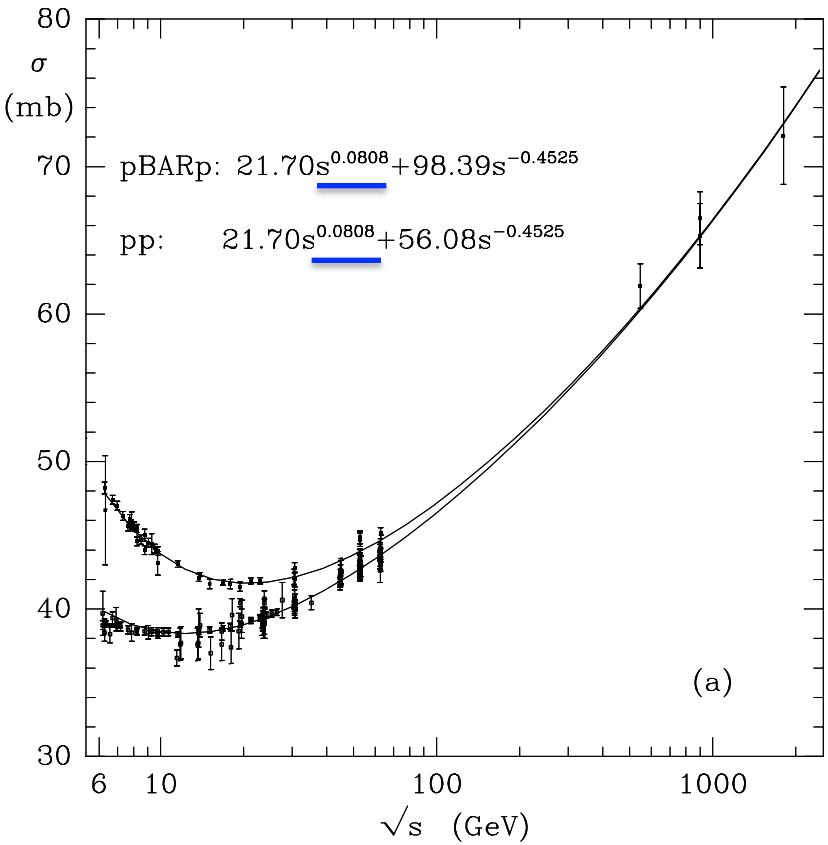

Donnachie and Landshoff (1992)

$\Delta = 0.0808$

$\sigma_{tot} \propto s^{\Delta}$ grows as a power function of s

Unitarity requires that the total cross section at very high energies should not grow faster than $\ln^2 s$ (Froissart bound).

DIFFRACTION: In HEP any process involving Pomeron exchange (theor. def.)

Optical theorem

$$\sum_c T_{ac} T_{ac}^* = 2\Im m T_{aa}$$

$\sigma_{tot} =$ 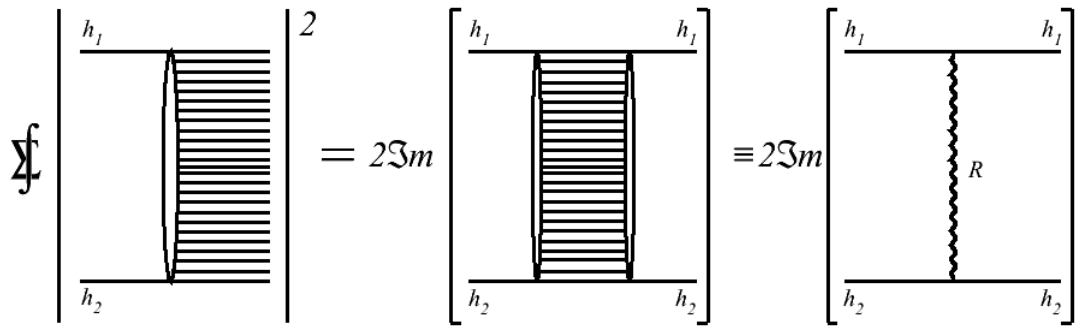

Analogous to the optical theorem, the Muller-Kancheli theorem relates the inclusive cross-section for the reaction $h_1+h_2 \to c+X$ to the forward scattering amplitude of the three-body hadronic process $h_1 + h_2 + \bar{c} \to h_1 + h_2 + \bar{c}$

single diff. = 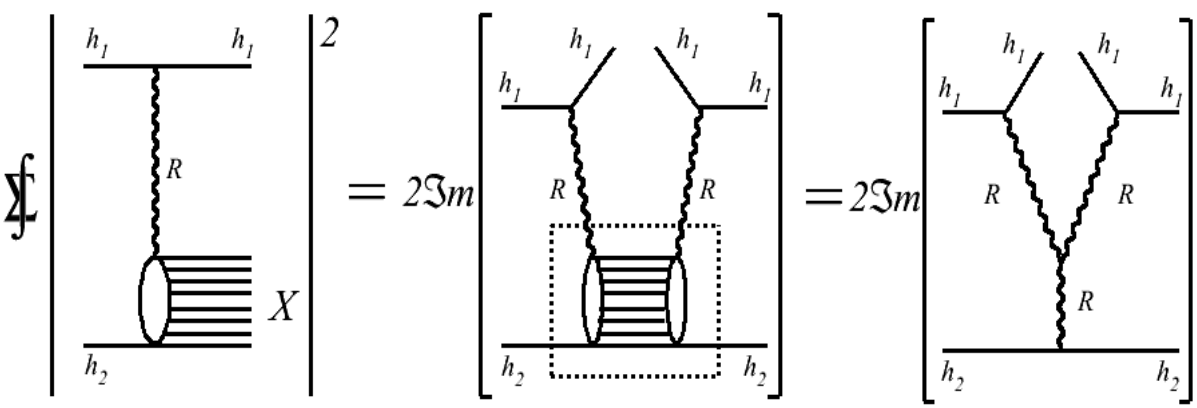

triple-Regge limit

1 GeV<<M_X <<$\sqrt{s}$

Triple-Regge diagram

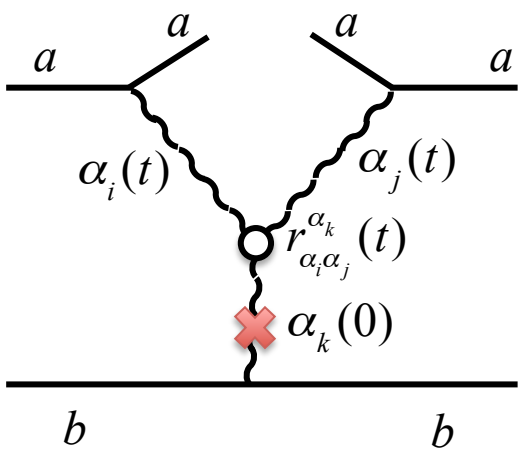

R: $\alpha_R(0) = 0.5$

P: $\alpha_P(0) = 1 + \Delta$

$$\frac{d\sigma^{(PP)P}}{dM} \propto \frac{s^{2\Delta}}{M^{1+2\Delta}}$$

$$\frac{d\sigma^{(PP)R}}{dM} \propto \frac{s^{2\Delta}}{M^{2+4\Delta}}$$

$$\frac{d\sigma_{SD}}{dM^2 dt} = \left(\frac{s_0}{s}\right)^2 \sum_{i,j,k} G_{ijk}(t) \left(\frac{s}{M^2}\right)^{\alpha_i(t)+\alpha_j(t)} \left(\frac{M^2}{s_0}\right)^{\alpha_k(0)}$$

•
•
•

Diffracted mass distribution in Pythia and Phojet

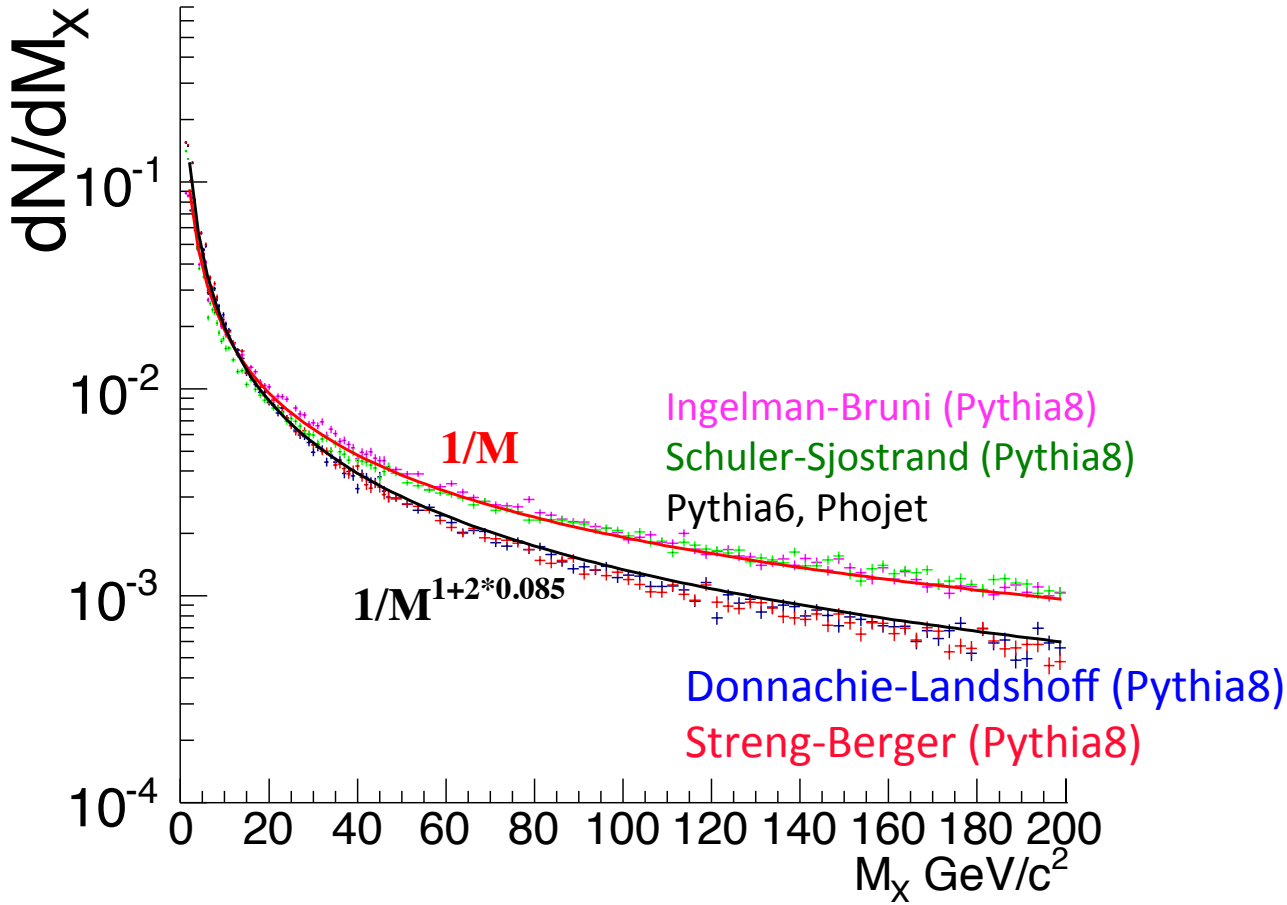

New implementation in Pythia8: MBR (Minimum Bias Rockefeller) arXiv:1205.1446

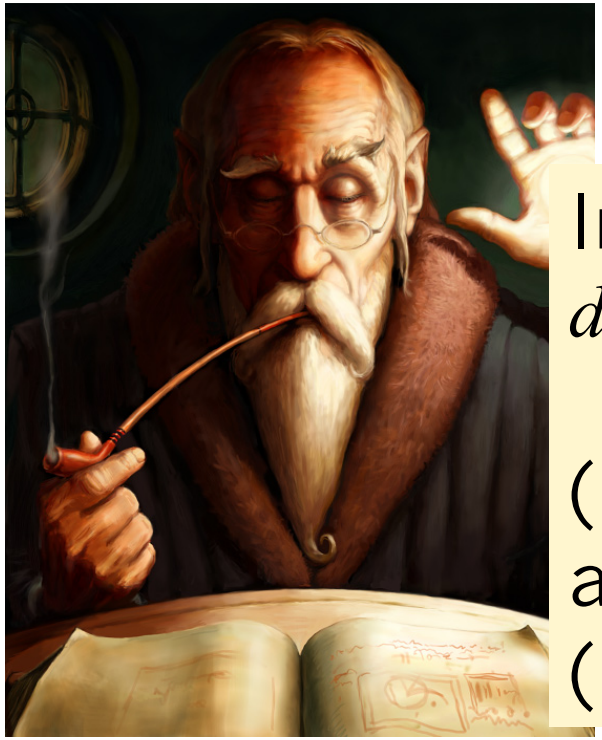

In MC (Pythia/Phojet) we have $d\sigma/dM \sim 1/M^{1+2\Delta}$.

(PP)R term behaves as $\sim 1/M^{2+4\Delta}$ and dominates at low masses (i.e. large gaps).

Reggeon Field Theory

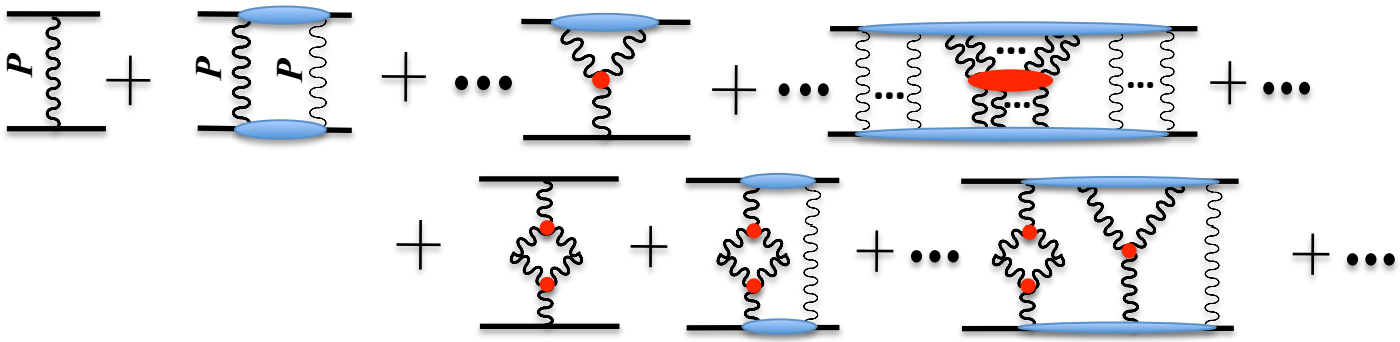

Gribov-1986

In the eikonal approximation (w/o enhanced graphs) $\sigma_{tot} \sim \ln^2 s \quad \text{at} \quad s >> m_N^2$

At high energies (parton densities) the interaction between Pomerons starts to play an important role.

Interaction vertices (multi-Pomeron and Pomeron-hadron) are not known theoretically.

models based on RFT:
Kaidalov-Ponomarev-Ter-Martirosyan, Khoze-Martin-Ryskin, Gotsman-Levin-Maor, Ostapchenko, Kaidalov-Poghosyan, ...

Main difference in implementing the GW mechanism, in used sets of diagrams, and in parameterizing interaction vertices (+AGK).

A model for describing high-mass diffractive dissociation in hh

Kaidalov and Poghosyan (2009)

All possible non-enhanced absorptive corrections to all legs of triple-Regge vertices diagrams

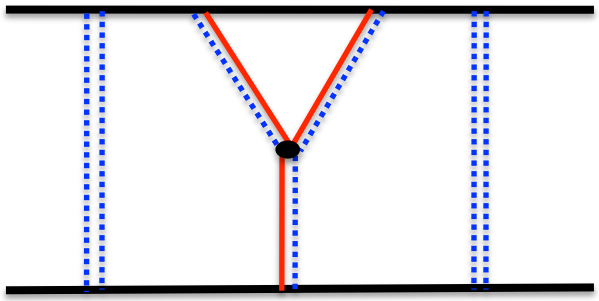

where

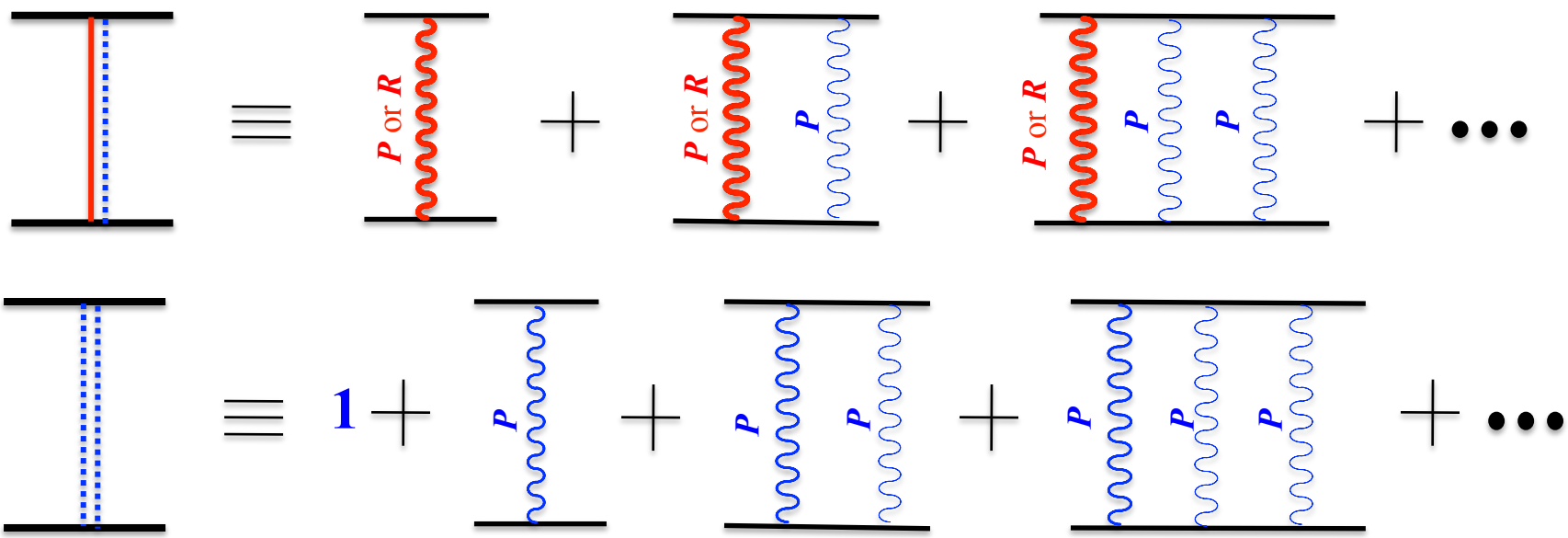

Fit to data on single diffraction dissociation

ISR: Armitage et al. NP B194

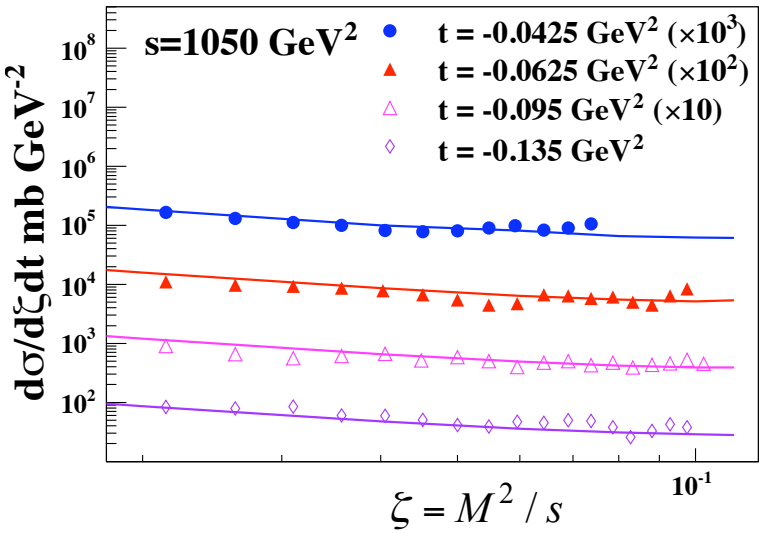

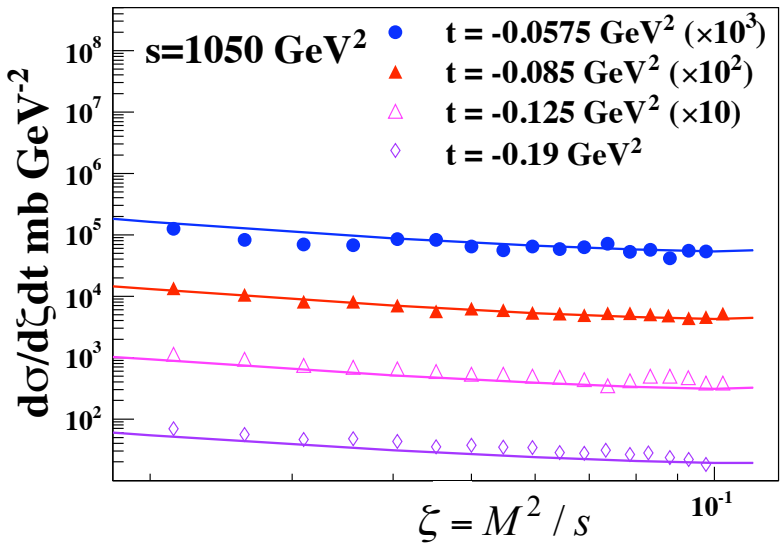

Akimov et al. PRL **39**

Cool et al. PRL **47**

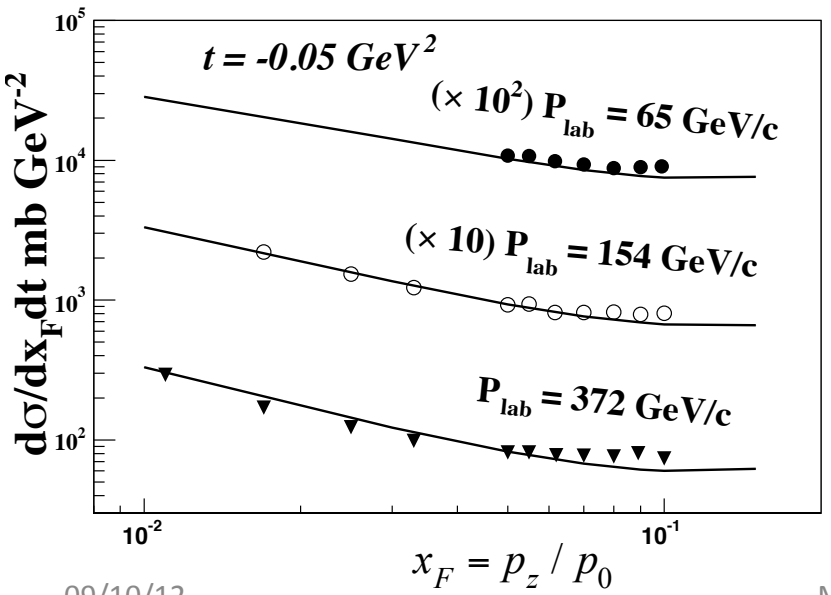

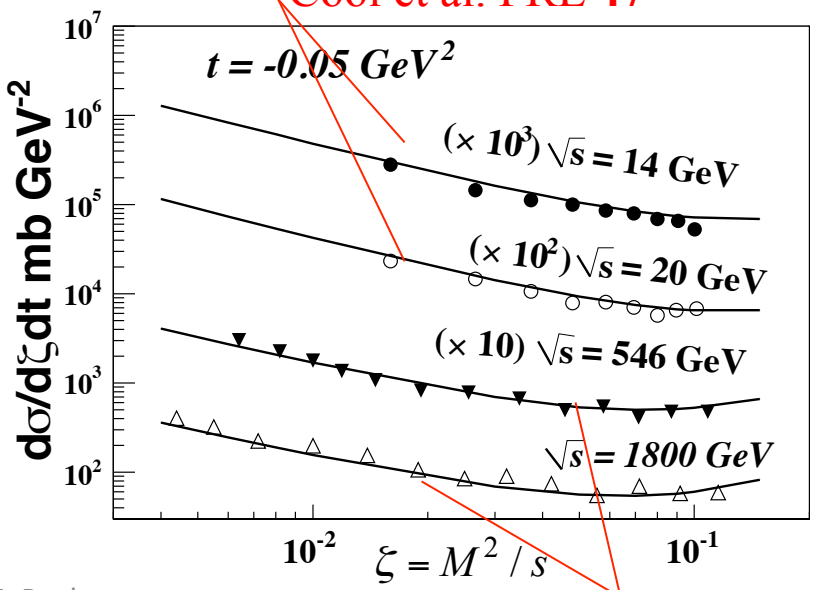

CDF:Goulianos, Montanha PR **D59**

SD mass distribution in MC simulation

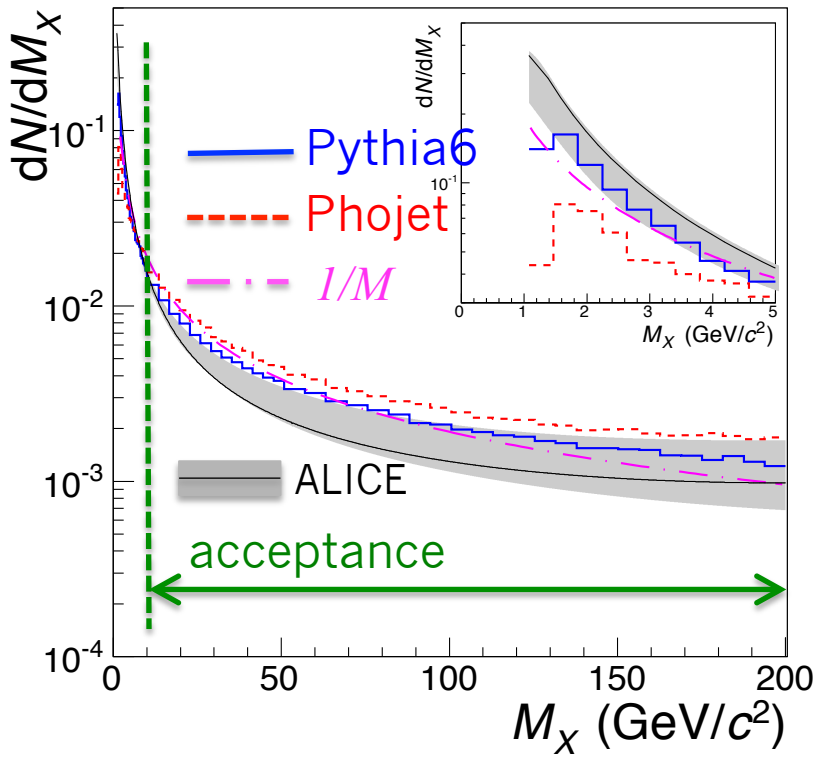

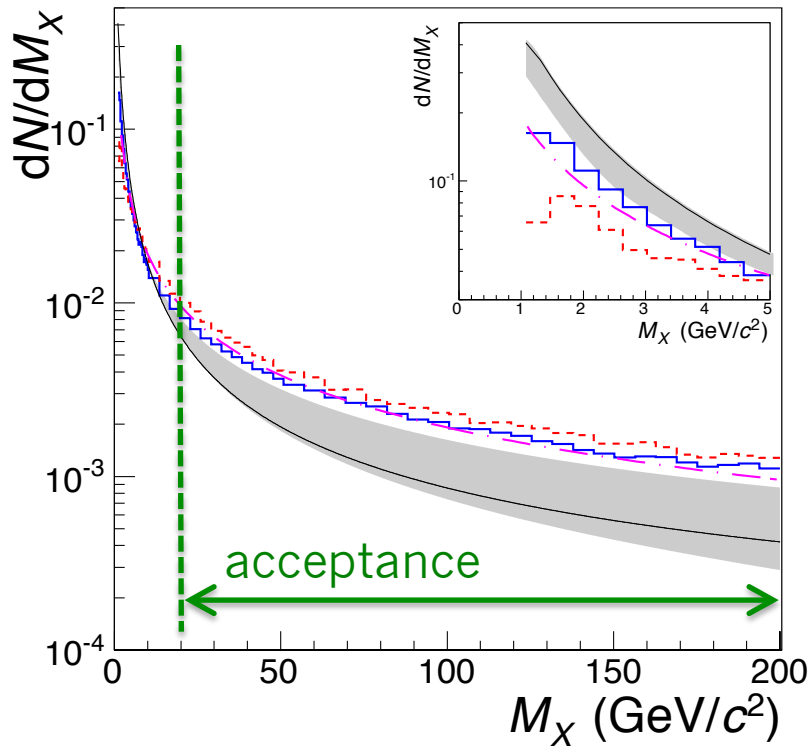

ALICE:
mean – KP model
syst – ±50% at min. mass +Donnachie-Landshoff

Topology of diffractive events

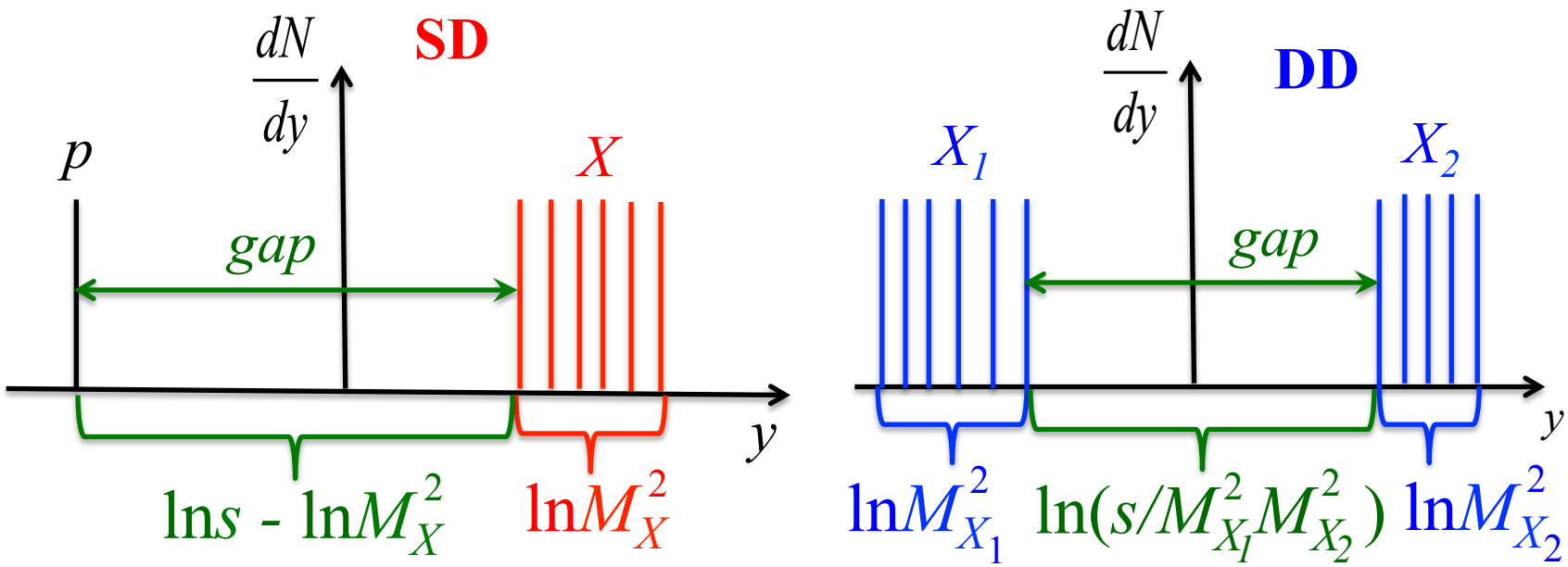

UA4 data on charged particle η-distribution in SD at √s = 546 GeV

D. Bernard et al, Phys. Lett. B166 (1986) 549.

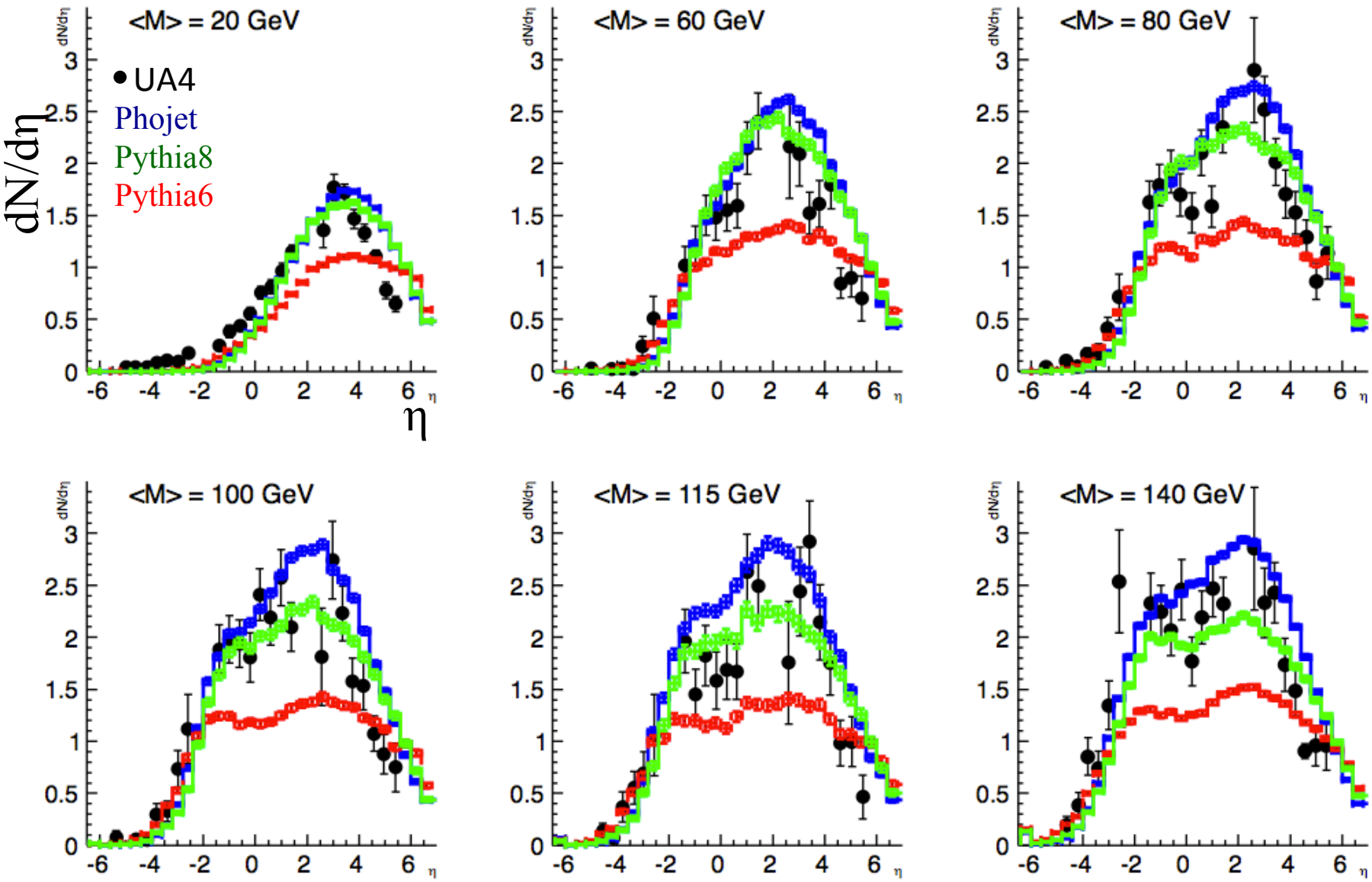

Let's look at the observed pseudorapidity gaps event-by-event and estimate the fraction of missed events with larger gaps.

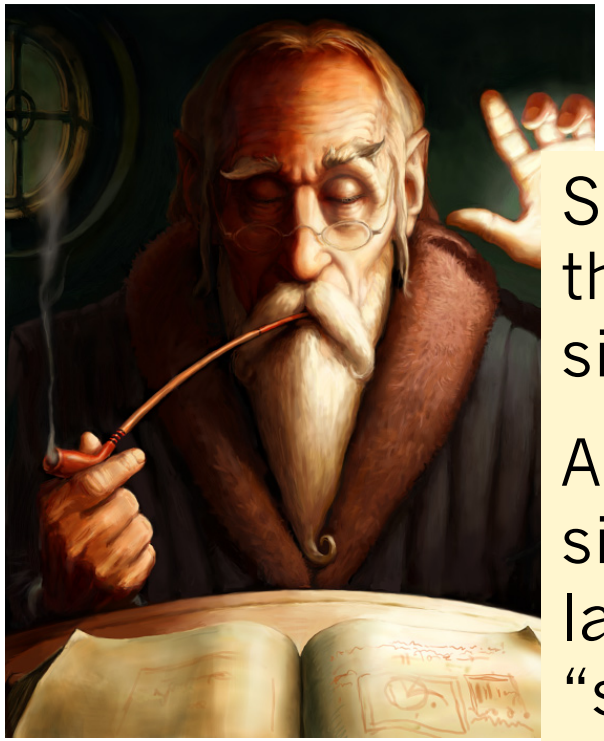

SD events are asymmetric. Let's measure their fraction by looking at the rate of single-arm triggers.

Asymmetric DD events may also give single-arm triggers. We looked at the largest η-gap distribution in measured "symmetric" event sample to constrain DD in MC and to estimate the fraction of DD events in single-arm triggers.

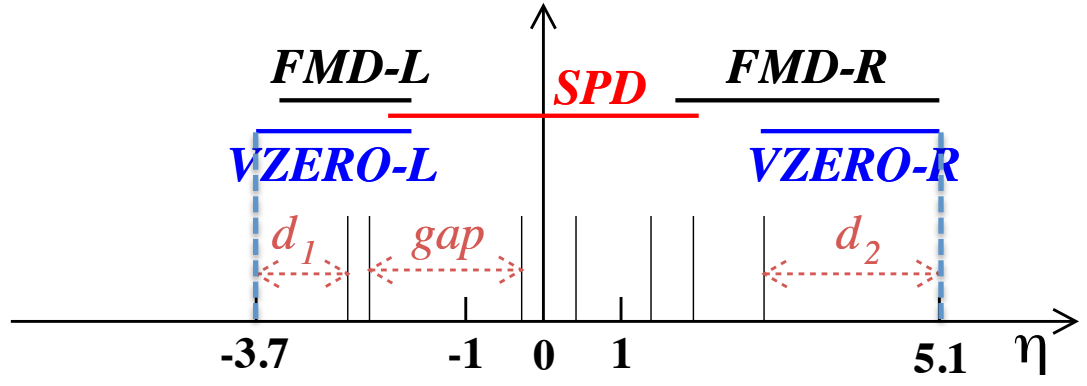

Definition of "Offline" triggers

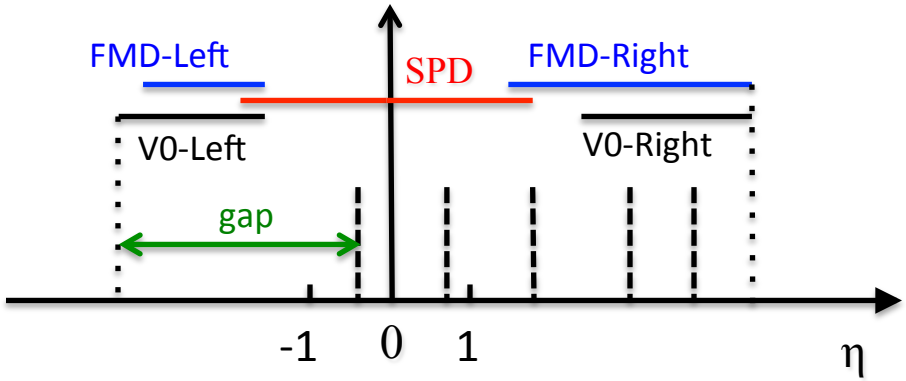

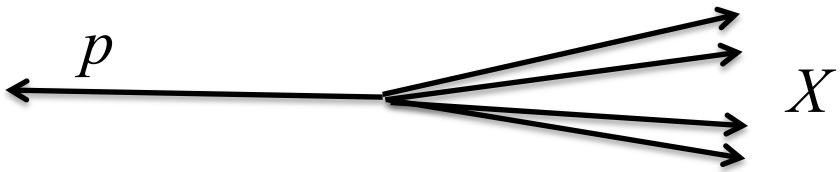

Right-side 1-arm trigger: no signal with $\eta < -1$

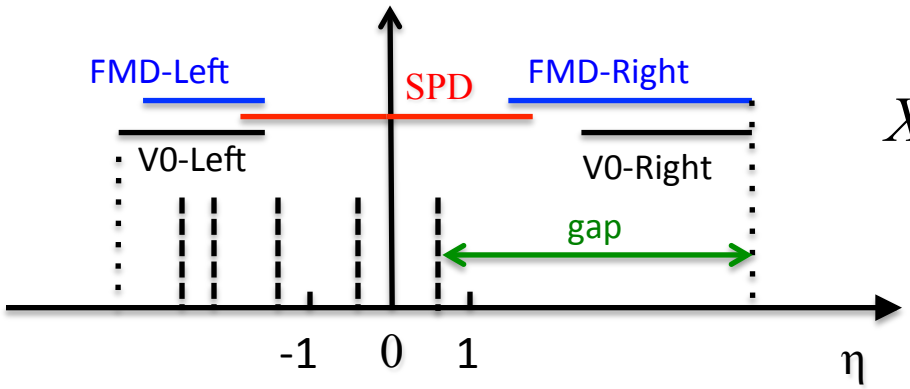

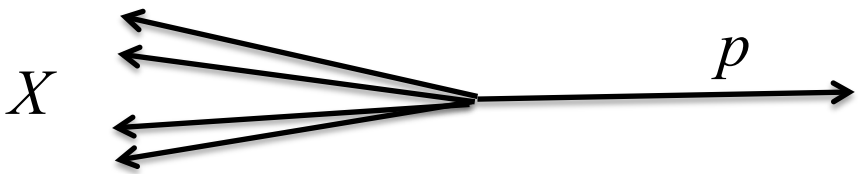

Left-side 1-arm trigger : no signal with $\eta > 1$

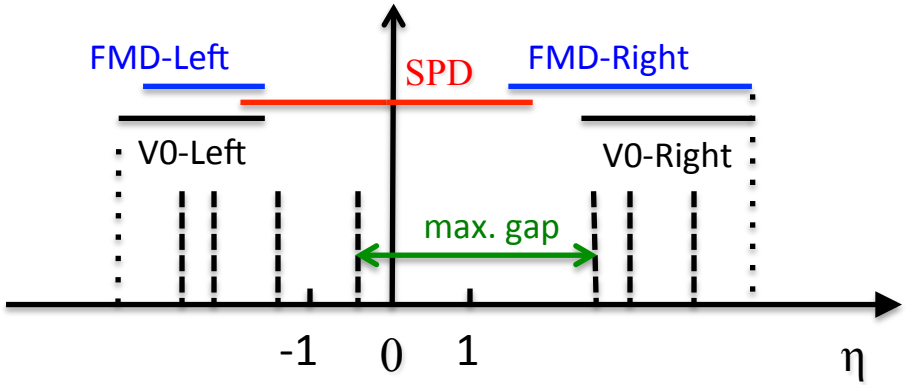

2-arm trigger

Varying the fraction of single- and double- diffractions in MC

The rate of 1-arm trigger is sensitive to SD

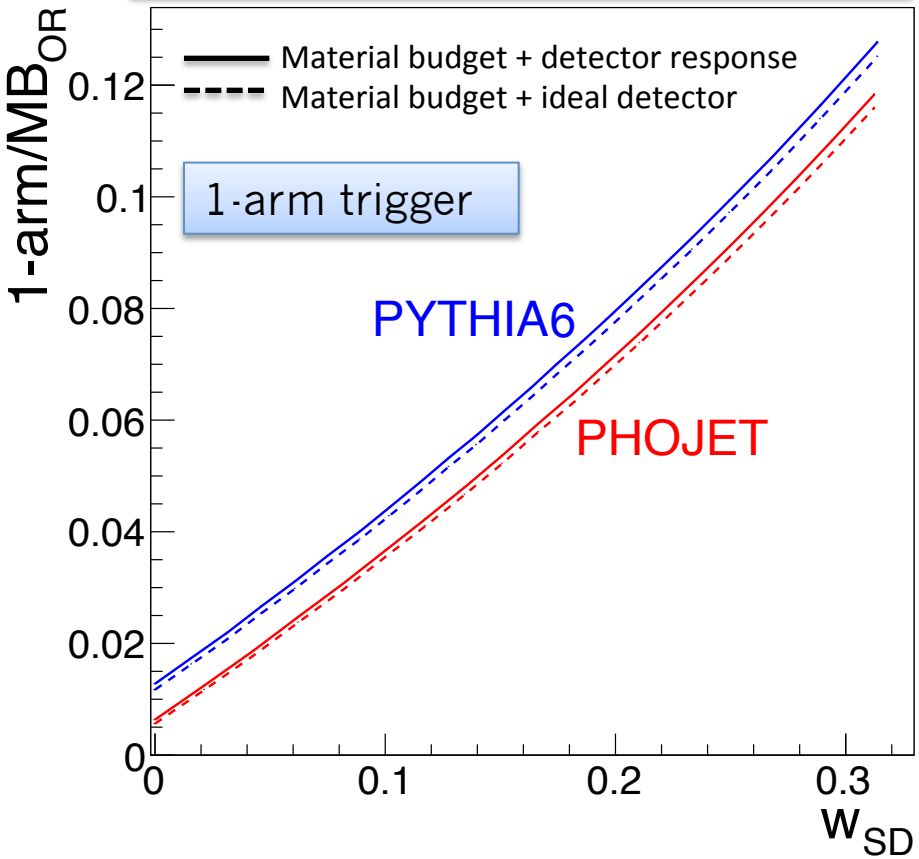

The gap width distribution is sensitive to DD

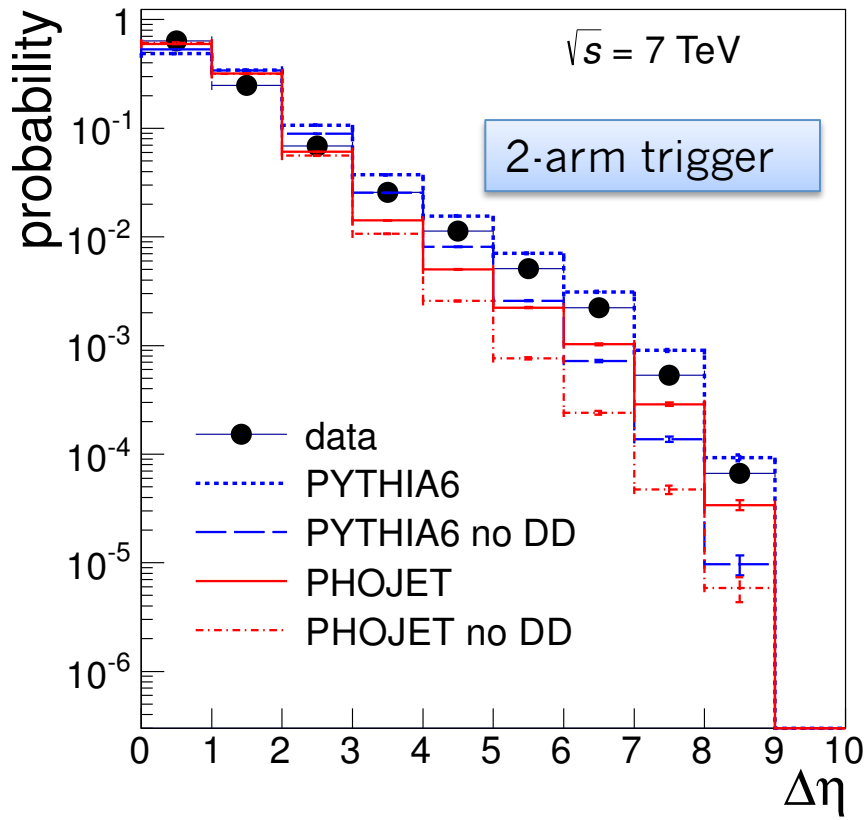

Material budget + simulation of detector response do not spoil the sensitivity to diffraction

Uncorrected data vs simulation with adjusted MC (7 TeV)

edge of left-side 1-arm trigger event

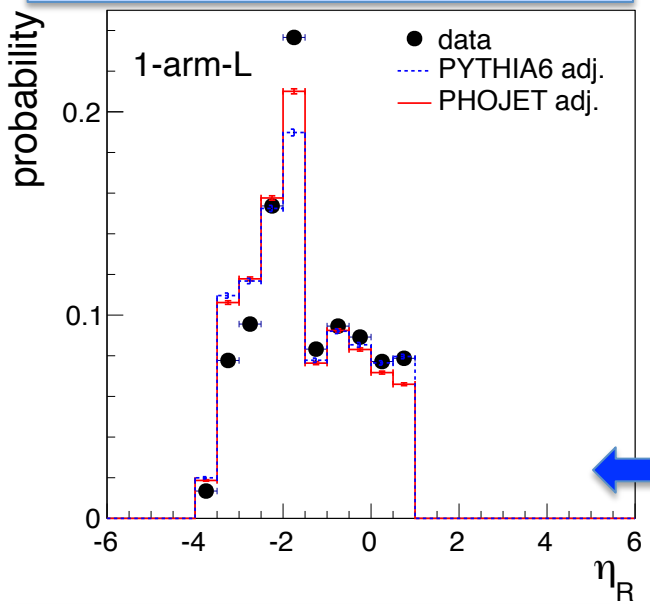

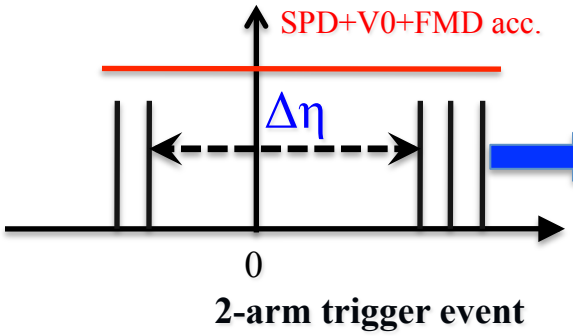

2-arm trigger

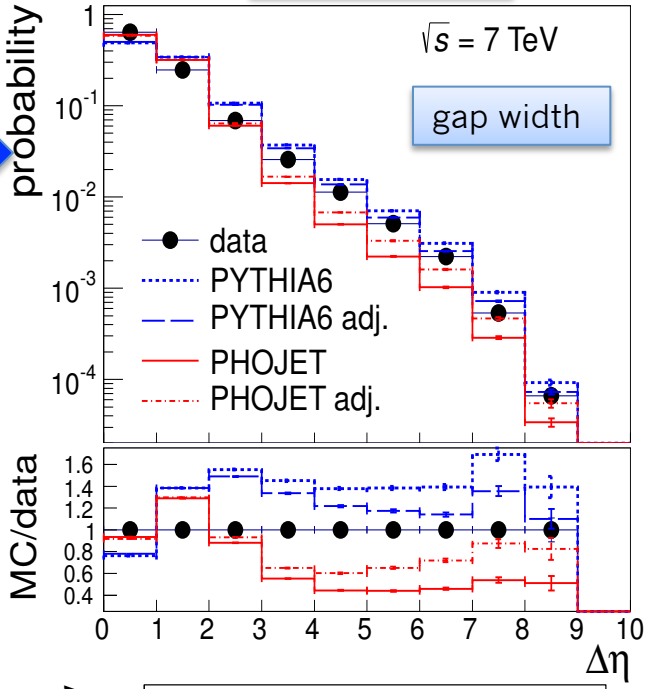

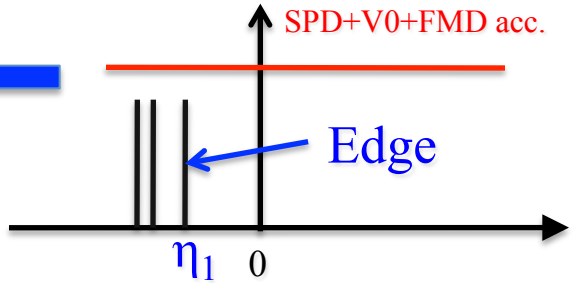

edge of right-side 1-arm trigger event

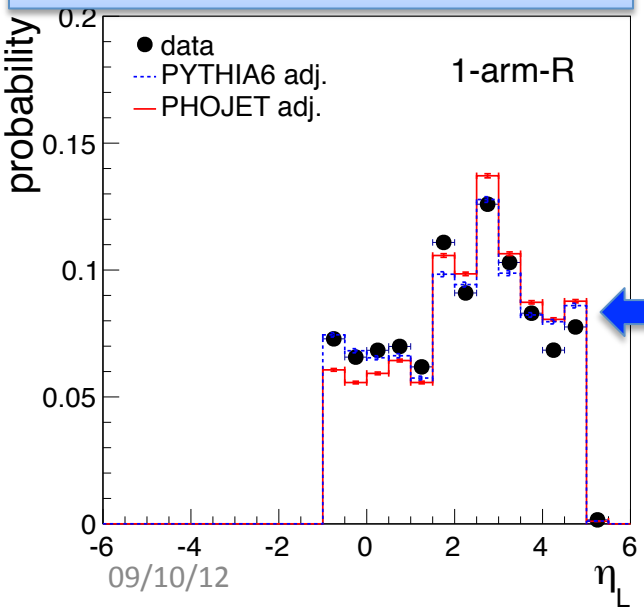

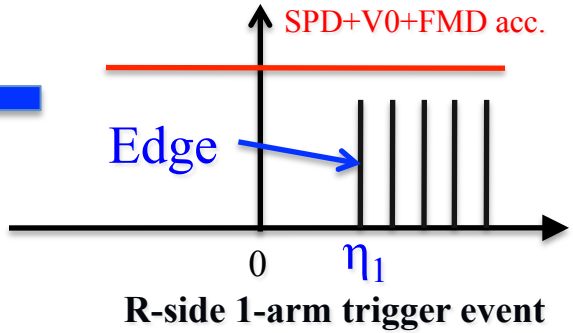

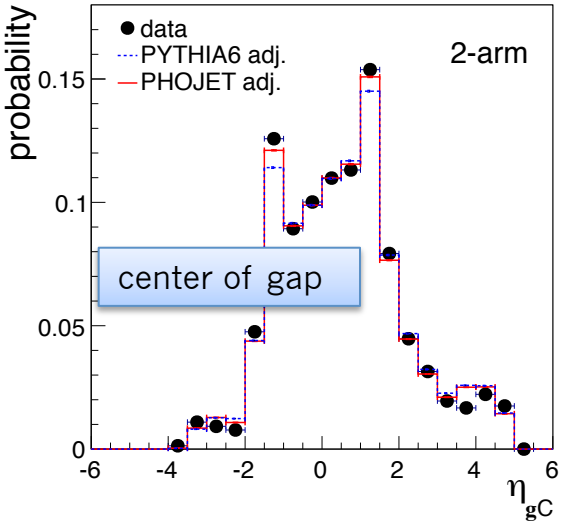

Done at 0.9 and 2.76 TeV

Trigger efficiency/inefficiency vs mass for SD

PYTHIA6

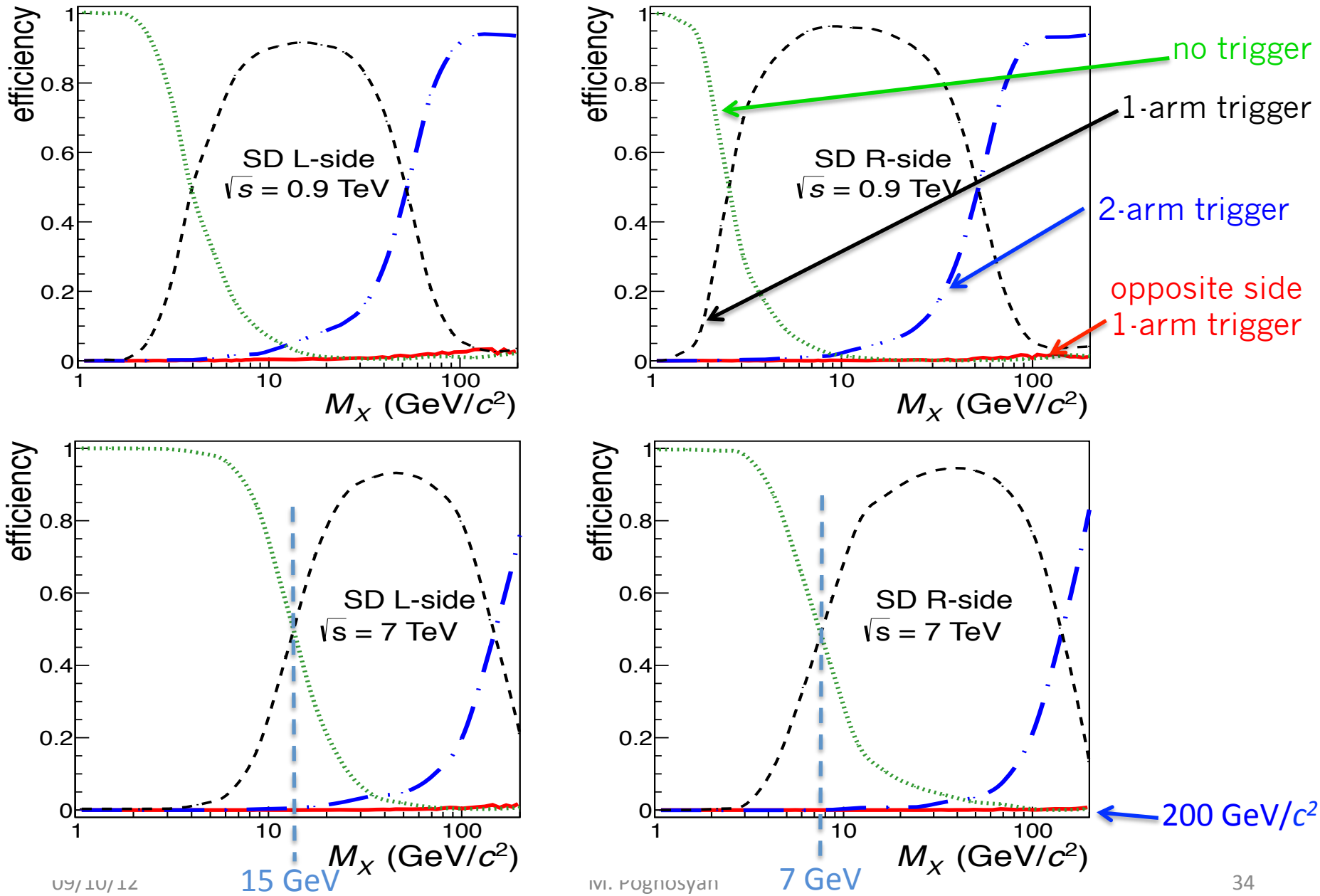

Raw trigger ratios and measurement of $\sigma_{SD}/\sigma_{Inel}$

fit to data with $A(\mu) = \left[\exp\{A_0\mu\} - 1\right] / \left[\exp\{\mu\} - 1\right]$

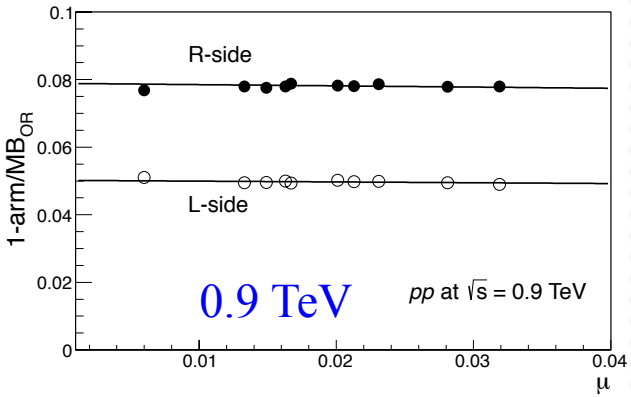

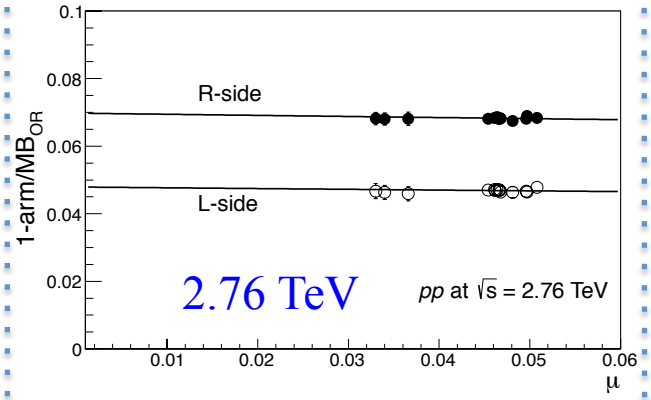

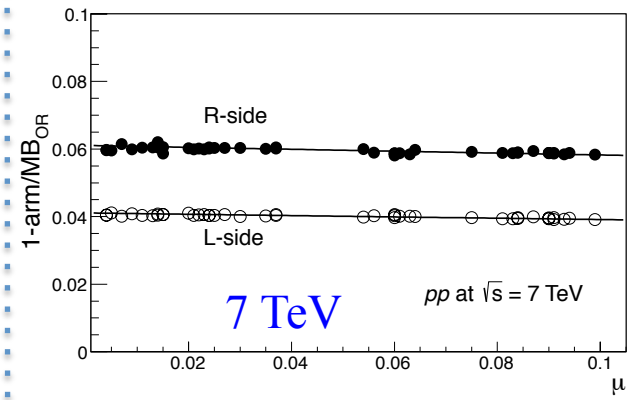

R-side/2-arm	$= 0.0906 \pm 0.0003$	0.0791 ± 0.0004	$0.0680 \pm negl.$
L-side/2-arm	$= 0.0576 \pm 0.0002$	0.0543 ± 0.0004	$0.0458 \pm negl.$

Corrected ratios

$\frac{\sigma_{SD}^{right}}{\sigma_{Inel}}$	$= 0.11 \pm 0.02$	$0.11^{+0.04}_{-0.05}$	$0.10^{+0.02}_{-0.03}$
$\frac{\sigma_{SD}^{left}}{\sigma_{Inel}}$	$= 0.10 \pm 0.02$	0.09 ± 0.03	$0.10^{+0.02}_{-0.04}$

The results are symmetrical as expected from the symmetry of the physics process.

$\frac{\sigma_{SD}}{\sigma_{Inel}}$	$= 0.21 \pm 0.03$	$0.20^{+0.07}_{-0.08}$	$0.20^{+0.04}_{-0.07}$

$\sigma_{SD}(M<200\ GeV/c^2)/\sigma_{INEL} \approx 0.2$ at all energies.

Triggering efficiencies

From adjusted MC we can calculate the ALICE trigger efficiencies:

MB_{OR} = V0-Left or SPD or V0-Right MB_{AND} = V0-Left and V0-Right

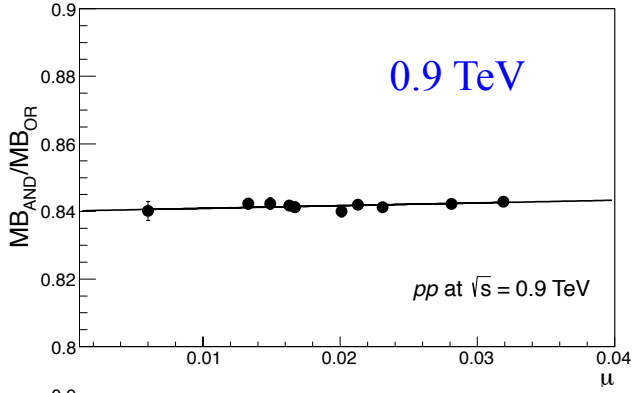

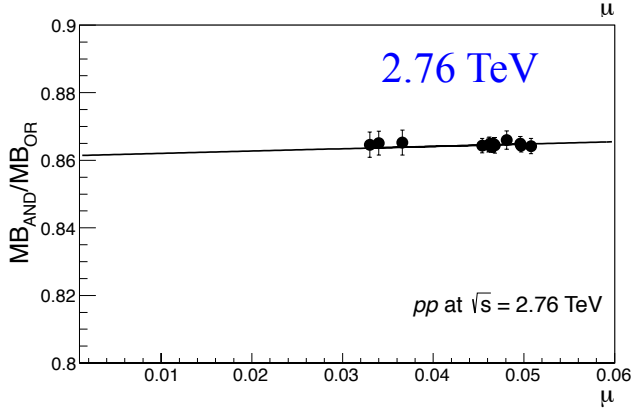

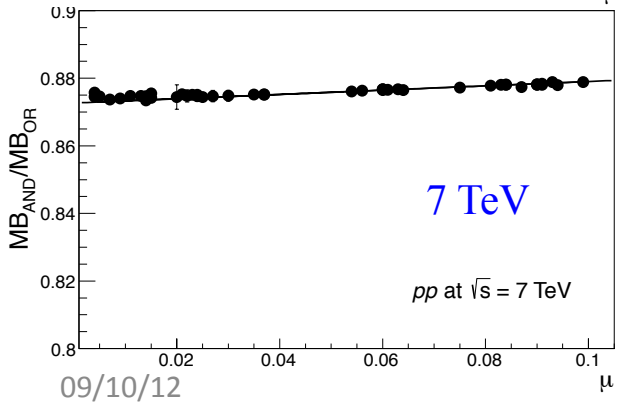

MC

$$MB_{AND} = 0.763 \; {}^{+0.022}_{-0.008}$$

$$MB_{OR} = 0.910 \; {}^{+0.032}_{-0.010}$$

$$\frac{MB_{AND}}{MB_{OR}} = 0.839 \; {}^{+0.006}_{-0.008}$$

Fit to data with $\alpha+0.5(1-\alpha)\mu$

0.840 ± *negl.*

$$MB_{AND} = 0.760 \; {}^{+0.052}_{-0.028}$$

$$MB_{OR} = 0.881 \; {}^{+0.059}_{-0.035}$$

$$\frac{MB_{AND}}{MB_{OR}} = 0.863 \; {}^{+0.020}_{-0.030}$$

0.861 ± *negl.*

$$MB_{AND} = 0.742 \; {}^{+0.050}_{-0.020}$$

$$MB_{OR} = 0.852 \; {}^{+0.062}_{-0.030}$$

$$\frac{MB_{AND}}{MB_{OR}} = 0.871 \; \pm 0.007$$

0.873 ± *negl*

$\sigma_{DD}/\sigma_{Inel}$

Using adjusted MC, we can obtain the rate of DD as a function of $\Delta\eta$

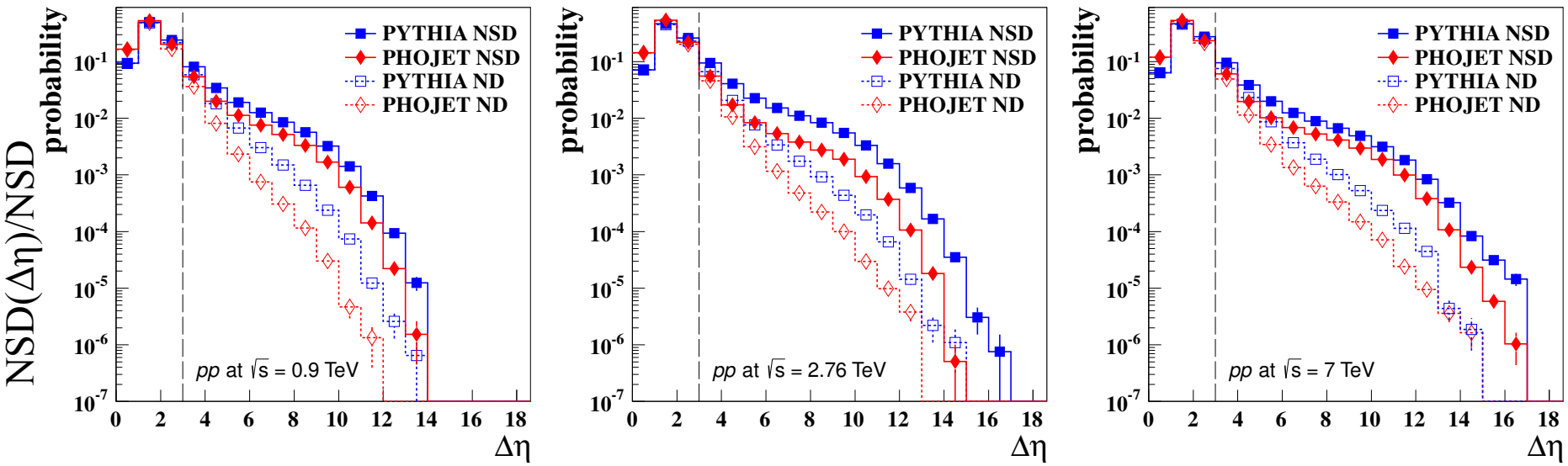

Definition of DD : all non-single diffractive events with a gap $\Delta\eta > 3$:

900 GeV

$$\frac{\sigma_{DD}}{\sigma_{Inel}} = 0.11 \quad \pm 0.03$$

2.76 TeV

$$\frac{\sigma_{DD}}{\sigma_{Inel}} = 0.12 \quad \pm \quad 0.05$$

7 TeV

$$\frac{\sigma_{DD}}{\sigma_{Inel}} = 0.12 \quad {}^{+0.05}_{-0.04}$$

$\Delta\eta > 3$ is chosen arbitrarily to allow comparison with other data

Van der Meer scans

An example: MB_{AND} trigger efficiency correction

A part of Inelastic cross-section is measured by requiring coincidence of V0-Left and V0-Right

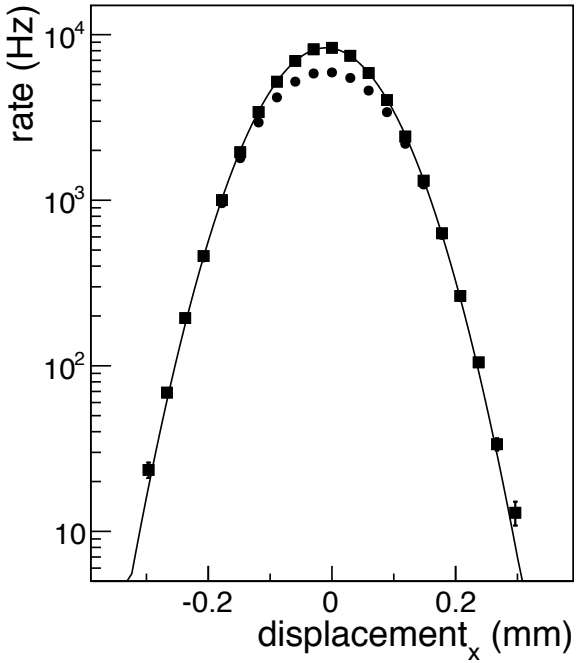

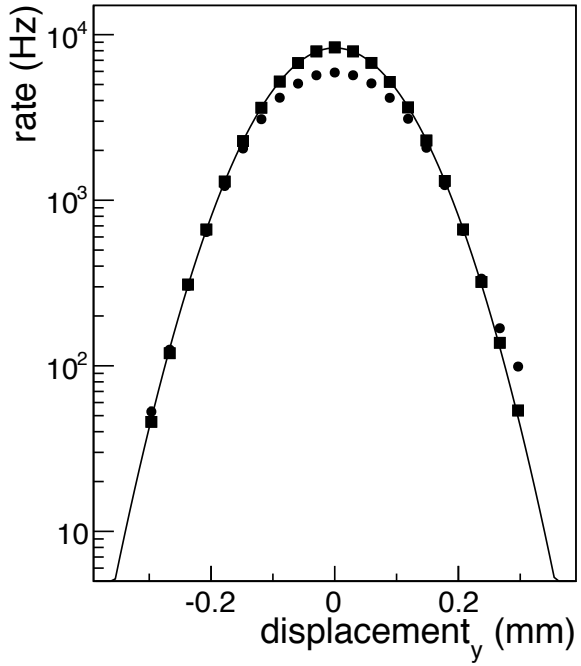

$$L = f\frac{N_1 N_2}{h_1 h_2}$$

f - accelerator frequency

$N_{1,2}$ – numbers of protons per bunch

h_x and h_y – effective width and height of the collision region

$$R^{trigger} = \sigma^{visible} \times L$$

$$\sigma_{INEL} = \frac{\sigma^{visible}}{\varepsilon}$$

$\sigma^{visible}$ ← vdM

ε ← MC

vdM scan	√s TeV	Colliding bunches	Crossing angle (rad)	β^* (m)	Max μ	$h_x/2\sqrt{\pi}$ (μm)	$h_y/2\sqrt{\pi}$ (μm)	$\sigma^{visible}$ (mb)	
1	7	1	280	2	0.086	44	47	54.2 ± 2.9	
2	7	1	500	3.5	0.74	58	65	54.3 ± 1.9	✓
3	2.76	48	710	10	0.12	158	164	47.7 ± 0.9	✓

Comparison with other experiments and models

σ_{INEL} at $\sqrt{s}$ = 7 TeV

With modeling of diffraction

ALICE : $73.2^{+2.0}_{-4.6}{}^{\text{model}} \pm 2.6^{\text{lumi}}$

ATLAS : $69.4 \pm 2.4^{\text{exp.}} \pm 6.9^{\text{extrap.}}$

CMS : $68.0 \pm 2.0^{\text{syst.}} \pm 2.4^{\text{lumi}} \pm 4^{\text{extrap.}}$

TOTEM: $73.5 \pm 0.6^{\text{stat.}}{}^{+1.8}_{-1.3}$ syst.

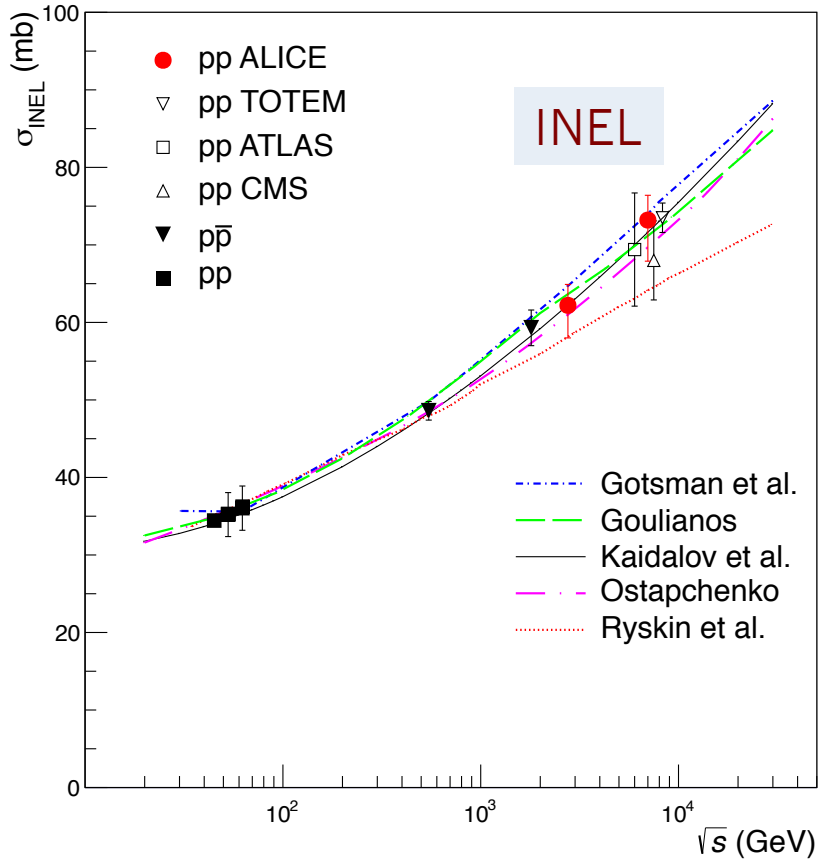

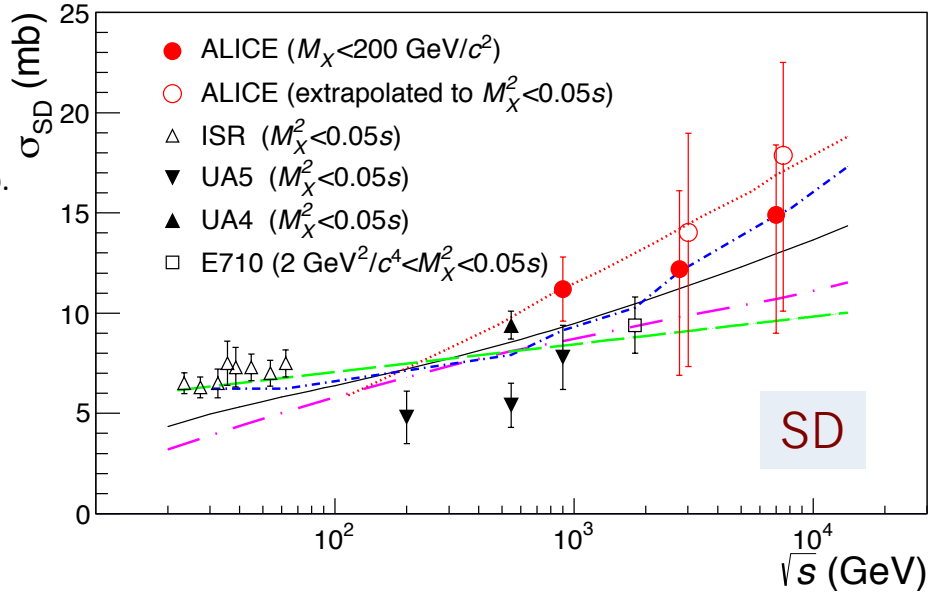

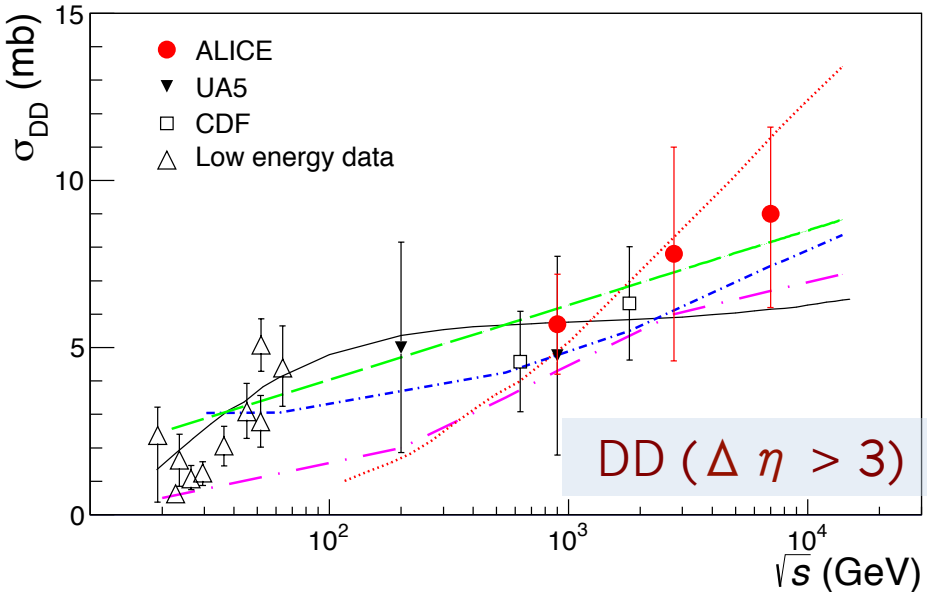

Consistency checks

- ✓ The two ALICE detector sides, which have different acceptances for diffracted masses (up to a factor 2 difference) gave consistent SD cross-section values, at three energies ($\sqrt{s}$ = 0.9, 2.76 and 7 TeV).

- ✓ The upper limit on the diffracted mass was changed to 50 and 100 GeV/c^2, and in each case the resulting observed cross-section followed the variation predicted by the KP model, a decrease by 20 % and 10 %, respectively.

- ✓ The run-to-run fluctuations and the small event pileup corrections were checked by using many runs with different pileup probabilities.

- ✓ The acceptance and efficiency calculations were checked indirectly by comparing measurements and MC simulations for MB_{AND}/MB_{OR} ratios.

- ✓ At $\sqrt{s}$ = 900 GeV, ALICE results were found to be consistent with UA5 data on $\sigma_{SD}/\sigma_{INEL}$ and $\sigma_{DD}/\sigma_{INEL}$ in $p\bar{p}$.

- ✓ At $\sqrt{s}$ = 7 GeV, ALICE result was found to be consistent with ATLAS result on σ_{INEL} for $M_{diff.}$ > 15.7 GeV.

  ALICE: $62.1^{+1.0}_{-0.9}(\text{syst}) \pm 2.2(\text{lumi})$ mb ATLAS: $60.3 \pm 0.5(\text{syst}) \pm 2.1(\text{lumi})$ mb

- ✓ The last word belongs to TOTEM: $\sigma_{INEL} = 73.5 \pm 0.6^{\text{stat.}}{}^{+1.8}_{-1.3}{}^{\text{syst.}}$ mb at 7TeV.

  ALICE: $73.2^{+2.0}_{-4.6}{}^{\text{model}} \pm 2.6^{\text{lumi}}$ (ALICE preliminary result became public before the TOTEM one).

Summary

Ratios of single-diffraction dissociation ($M < 200$ GeV/c^2) to inelastic cross-sections were measured at $\sqrt{s}$ = 0.9, 2.76 and 7 TeV. Within measurement accuracy, no variation of these ratios with energy was observed ($\sigma_{SD}/\sigma_{INEL} \approx 0.2$).

This allowed a determination of the inelastic cross-section, and of single-diffraction and double-diffraction cross-sections.

$\sqrt{s}$ (TeV)	σ_{INEL} (mb)	σ_{SD}(M < 200 GeV) (mb)	$\sigma_{DD}(\Delta\eta>3)$ (mb)
0.9	$52.5^{+2.0}_{-3.3}$*	$11.2^{+1.6}_{-2.1}$	5.6 ± 2.0
2.76	$62.8^{+2.4}_{-4.0} \pm 1.2$	$12.2^{+3.9}_{-5.3}$	7.8 ± 3.2
7	$73.2^{+2.0}_{-4.6} \pm 2.6$	$14.9^{+3.4}_{-5.9}$	9.0 ± 2.6

* No vdM scan at 0.9 TeV. Based on cross-section measurement by UA5.

EUROPEAN ORGANIZATION FOR NUCLEAR RESEARCH

CERN-PH-EP-2012-138
August 27, 2012

Measurement of inelastic, single- and double-diffraction cross sections in proton–proton collisions at the LHC with ALICE

The ALICE Collaboration

e-Print: arXiv:1208.4968 [hep-ex]

Thank you